Award Number: W81XWH-10-1-0749

TITLE:
BRMS1 suppresses breast cancer metastasis to bone via its regulation of microRNA-125b and downstream attenuation of TNF-alpha and HER2 signaling pathways.

PRINCIPAL INVESTIGATOR:
Yekaterina B. Khotskaya, Ph.D.

CONTRACTING ORGANIZATION:
University of Texas MD Anderson Cancer Center
Houston, TX 77030

REPORT DATE: October 2013

TYPE OF REPORT: Annual Summary

PREPARED FOR: U.S. Army Medical Research and Materiel Command
Fort Detrick, Maryland 21702-5012

REPORT DOCUMENTATION PAGE

Form Approved
OMB No. 0704-0188

1. REPORT DATE	2. REPORT TYPE	3. DATES COVERED
October 2013	Annual Summary	29September2012–28September2013

4. TITLE AND SUBTITLE
BRMS1 suppresses breast cancer metastasis to bone via its regulation of microRNA-125b and downstream attenuation of TNF-alpha and HER2 signaling pathways

5a. CONTRACT NUMBER
W81XWH-10-1-0749

5b. GRANT NUMBER
W81XWH-10-1-0749

5c. PROGRAM ELEMENT NUMBER

5d. PROJECT NUMBER

5e. TASK NUMBER

5f. WORK UNIT NUMBER

6. AUTHOR(S)
Yekaterina B. Khotskaya and Mien-Chie Hung

E-Mail: ybkhotskaya@mdanderson.org

7. PERFORMING ORGANIZATION NAME(S) AND ADDRESS(ES)
University of Texas MD Anderson Cancer Center
1515 Holcombe Blvd
Unit 108
Houston, TX 77030

8. PERFORMING ORGANIZATION REPORT NUMBER

9. SPONSORING / MONITORING AGENCY NAME(S) AND ADDRESS(ES)
U.S. Army Medical Research and Materiel Command
Fort Detrick, Maryland 21702-5012

10. SPONSOR/MONITOR'S ACRONYM(S)

11. SPONSOR/MONITOR'S REPORT NUMBER(S)

12. DISTRIBUTION / AVAILABILITY STATEMENT
Approved for Public Release; Distribution Unlimited

13. SUPPLEMENTARY NOTES

14. ABSTRACT
Human breast cancer cells with restored BRMS1 expression exhibit few *in vitro* changes when compared to control cells, but demonstrate a very strong suppression of metastasis in *in vivo* animal models of breast cancer and several other solid tumor types. We have previously shown that in tissue samples collected from breast cancer patients, there exists an inverse correlation between expression of BRMS1 and HER2, an important druggable target in breast cancer. HER2 expression and function are particularly important in the context of inflammatory breast cancer, where up to 60% of all tumors are HER2+, but usually negative for hormone receptors ER and PR. Patients with inflammatory breast cancer have few treatment options and have one of the highest metastatic relapse rate and lowest survival among all breast cancer patients. In Year 1 progress report, we identified KPL4 inflammatory breast cancer cell line as a good candidate for re-expression of BRMS1, since there is HER2 amplification and cells were described in the literature as spontaneously metastatic. In the studies described below, we identified several novel BRMS1-interacting partners, such as AMPK, a major kinase regulating cellular metabolism, and Filamin B, a cytoplasmic protein that participates in cellular adhesion and motility. We also determined that BRMS1 can be phosphorylated on a single Serine residue and that this phosphorylation sites lies within an AMPK consensus sequence. Finally, we determined that BRMS1-expressing cells exhibit a decreased level of phosphorylated STAT3, leading to modulation in expression of pro-apoptotic genes. However, based on new data, we identified a non-cononical mechanism responsible for decreased STAT3 phosphorylation.

15. SUBJECT TERMS
BRMS1, metastasis, bone

16. SECURITY CLASSIFICATION OF: U			17. LIMITATION OF ABSTRACT	18. NUMBER OF PAGES	19a. NAME OF RESPONSIBLE PERSON
a. REPORT	b. ABSTRACT	c. THIS PAGE			USAMRMC
U	U	U	UU	26	19b. TELEPHONE NUMBER *(include area code)*

Table of Contents

1. Introduction

Human breast cancer cells with restored BRMS1 expression exhibit few *in vitro* changes when compared to control cells, but demonstrate a very strong suppression of metastasis in *in vivo* animal models of breast cancer and several other solid tumor types. We have previously shown that in tissue samples collected from breast cancer patients, there exists an inverse correlation between expression of BRMS1 and an epidermal growth factor receptor 2 (HER2) [1], an important "druggable" target in breast cancer. HER2 expression and function are particularly important in the context of inflammatory breast cancer, where up to 60% of all tumors are HER2+, while they are usually negative for hormone receptors ER and PR [2]. Patients with inflammatory breast cancer have few treatment options and have one of the highest metastatic relapse rate and lowest survival among all breast cancer patients [2]. In Year 1 progress report, we identified KPL4 inflammatory breast cancer cell line as a good candidate for re-expression of BRMS1, since KPL4 cells exhibit a 15-fold HER2 amplification and the cells were described in the literature as spontaneously metastatic [3]. In Year 2, we went on to show that BRMS1 expression in these cells inhibits cell adhesion to several matrices, and preferentially suppresses metastasis to bone. We also began to investigate molecular mechanisms responsible for inhibition of metastasis and identified Stat3 signaling as a potential driver signaling cascade. In the current report, we identified several novel BRMS1-interacting partners, such as AMPK, a major kinase regulating cellular metabolism, and Filamin B, a cytoplasmic protein that participates in cellular adhesion and motility. We also determined that BRMS1 can be phosphorylated on a single serine residue, S237, and that this phosphorylation site lies within an AMPK consensus sequence. Finally, we determined that BRMS1-expressing cells exhibit a decreased level of phosphorylated STAT3, leading to modulation in expression of pro-apoptotic genes. Based on our new data, we identified a non-cononical mechanism that might be responsible for this decreased STAT3 phosphorylation.

Progress related to Aim 1 (Tasks 1.1 through 1.4) was described in previous yearly reports and more recently in a publication in *Molecular Carcinogenesis* (see Appendix 2). Therefore, it will not be discussed further in this progress report. Here, we will describe our progress during Year 3 on tasks 2.2, 2.3, 2.4, and 2.5.

2. Results

Tasks 2.2-2.3. During Year 2, we performed mass spectrometry analysis of protein complexes co-immunoprecipitated with BRMS1. The top 14 proteins that associate with BRMS1 are shown in Fig. 1A. Of these BRMS1-interacting partners, many were shown to bind BRMS1 previously, but we were excited to see two novel binding partners, 5' AMP-activated protein kinase (AMPK) and Filamin B, an actin binding protein that plays a role in cell spreading. Based on mass spectrometry data, we then immunoprecipitated BRMS1 and confirmed its interaction with Filamin B and AMPK (Fig. 1B). HDAC1 was included as a positive control for immunoprecipitation, as BRMS1 had been shown previously to associate with many HDAC proteins [4]. Finally, mass spectrometry analysis revealed that BRMS1 expressed in KPL4 breast cancer cells undergoes phosphorylation on a single site, serine 237 (Fig. 1C). This serine is localized within the AMPK consensus sequence [5], which suggests that BRMS1 might be phosphorylated by AMPK.

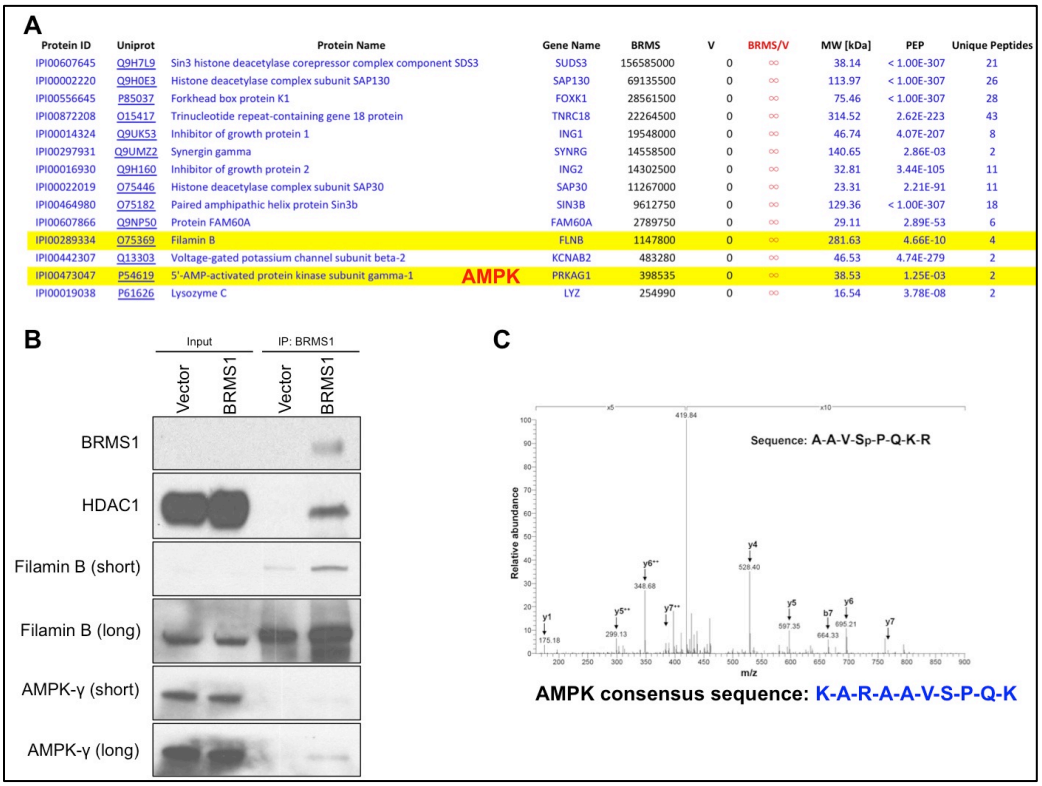

Figure 1. A: List of top 14 BRMS1-interacting proteins identified by mass spectrometry. Filamin B and AMPK (highlighted in yellow) are novel BRMS1 interacting partners. B: Immunoprecipitation of BRMS1 from KPL4-vector and KPL4-BRMS1 cells confirms interaction between BRMS1 and Filamin B, and BRMS1 and AMPK-gamma. C: Mass spectrometry identified a single phosphorylated residue within BRMS1, serine 237. This serine residue lies within an AMPK consensus sequence (in blue).

AMPK is one of the major enzymes that regulate cellular metabolism, and it exists as a heterotrimer that consists of an alpha, a beta, and a gamma subunit [6]. The alpha subunit carries out the AMPK catalytic function and is responsible for phosphorylation of the AMPK substrates [7], while the beta and gamma subunits play a regulatory role. Specifically, the gamma subunit is thought to bind AMP, causing a conformational change in the AMPK trimer and affecting its function [8]. Our data indicated that BRMS1 binds specifically to the gamma subunit of AMPK (Fig. 1A-B). Nonetheless, AMPK is a kinase with many known substrates and the phosphorylation on BRMS1 that we identified lies within the AMPK consensus sequence. Thus, we then performed an in vitro kinase assay using purified AMPK and BRMS1 proteins. Data in Fig. 2A show that AMPK phosphorylates BRMS1; however, it is not clear if AMPK phosphorylates BRMS1 on S237 that we identified by mass spectrometry.

In order to determine if phosphorylation of BRMS1 on serine 237 carries a biological function, we then mutated serine 237 to alanine (S237A), which represents a non-phosphorylatable mimetic of BRMS1 protein. Upon expression of wild-type BRMS1 or S237A BRMS1 in KPL4 and MDA-231 breast cancer cells, we determined that both constructs are expressed to a similar level (Fig. 2B) and that this mutation in BRMS1 sequence does not affect its nuclear localization, where BRMS1 is thought to carry out its functions (Fig. 2C).

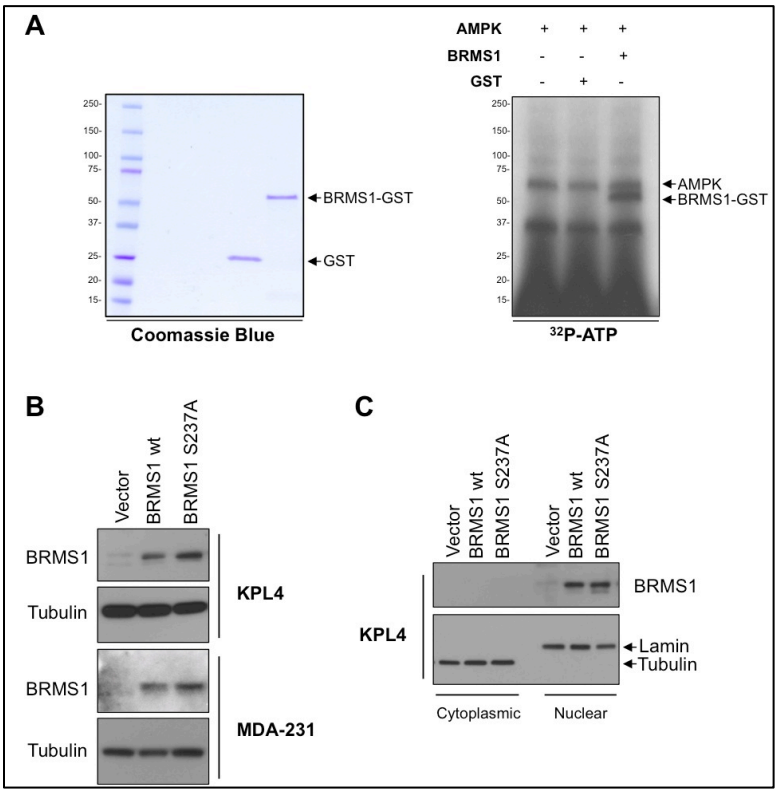

Figure 2. A: AMPK phosphorylates BRMS1 in an in vitro kinase assay. B: Wild-type and S237A mutant BRMS1 are expressed at a similar level in KPL4 and MDA-231 breast cancer cells. C: Expression of S237A BRMS1 mutant does not affect cellular localization of BRMS1.

As mentioned previously, during Year 2 of funding, we identified that expression of BRMS1 inhibits phosphorylation of STAT3 transcription factor. Therefore, we then examined whether S237A mutation played a role in this phenomenon. As shown in Fig. 3A, expression of the mutated BRMS1 reversed inhibition of STAT3 phosphorylation. We then hypothesized that signaling through one of the pathways upstream of STAT3 must be inhibited by BRMS1 expression. However, data revealed that signaling through JAK, IGF1R, and SRC pathways, which constitute canonical signaling, was not reduced in BRMS1-expressing KPL4 cells (Fig. 3B-C). Recent breakthroughs in the understanding of STAT3 regulation exposed a fine balance between STAT3 acetylation, phosphorylation, and its ability to induce transcriptional changes of STAT3-driven genes [9]. Specifically, p300 is known to acetylate STAT3 and correlates with enhanced STAT3 phosphorylation, while HDAC1/2 de-acetylate STAT3 and reduce its transcriptional ability [10]. Since BRMS1 is know to associate with and promote activity of several HDAC proteins [4], we then hypothesized that STAT3 might be de-acetylated in BRMS1-expressing cells. As shown in Fig. 3D, we immunoprecipitated proteins that are lysine acetylated using a pan acetyl-lysine antibody. While we detected a clear band corresponding to STAT3 in vector KPL4 cells, this band was absent in pull-down sample from BRMS1-expressing KPL4 cells. In the future, we plan to determine whether S237A mutation reverses this phenomenon, as would be predicted based on STAT3 phosphorylation results shown above (Fig. 3A)

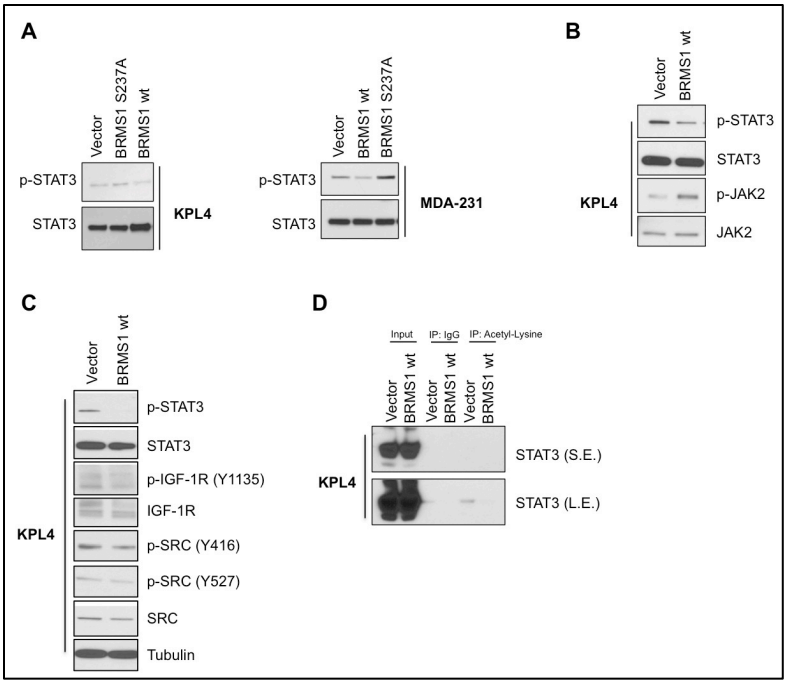

Figure 3. A: S237A mutation in BRMS1 reverts BRMS1-mediated inhibition in STAT3 phosphorylation. B-C: Expression of wild-type BRMS1 does not inhibit signaling through canonical pathways upstream of STAT3. D: STAT3 acetylation is greatly reduced in BRMS1-expressing KPL4 cells.

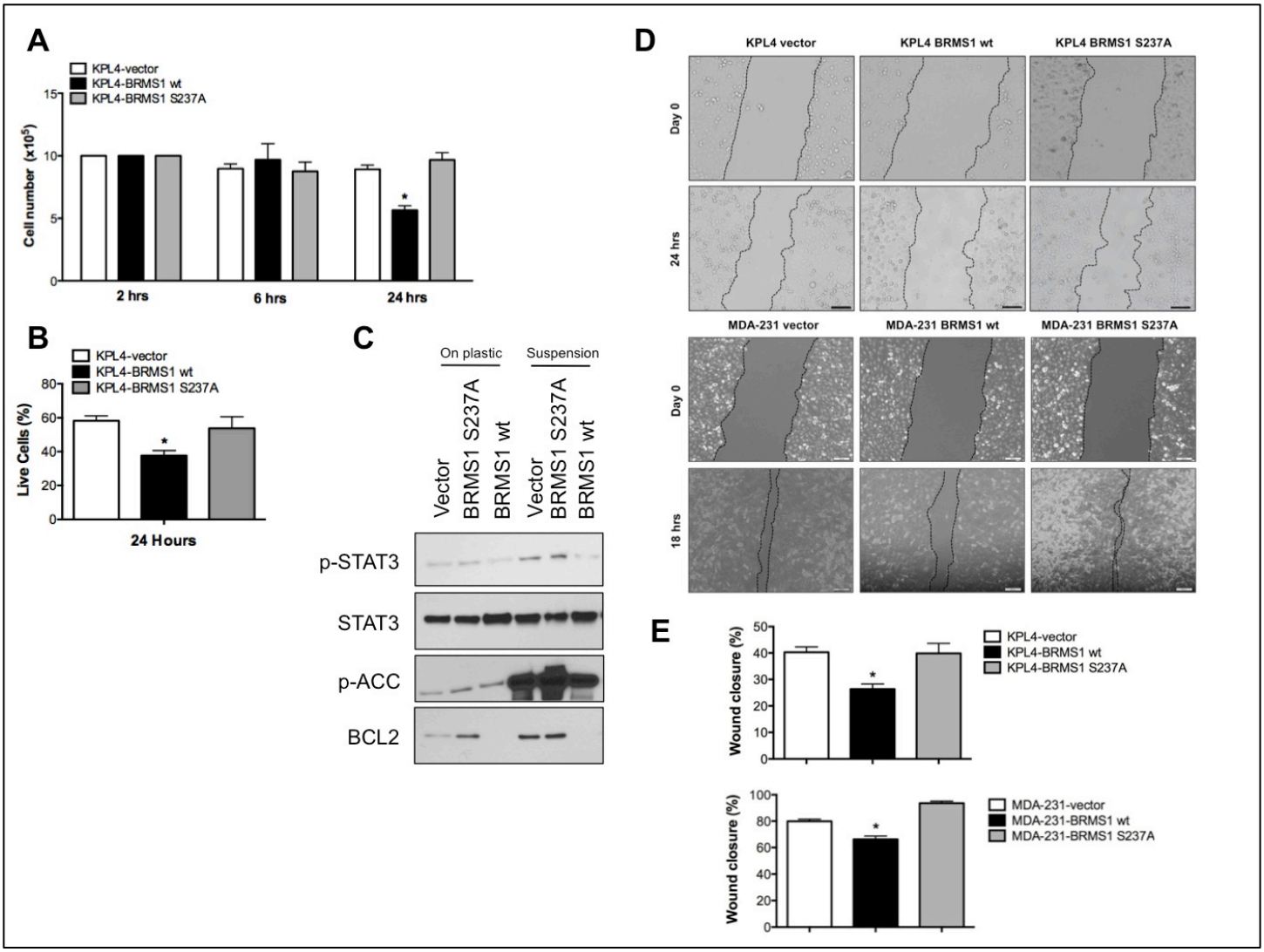

Figure 4. A-B: Expression of wild-type, but not S237A mutant BRMS1, induces anoikis of KPL4 cells. C: Anoikis conditions activate AMPK and enhance STAT3 phosphorylation in vector and S237A-expressing KPL4 cells, but not in cells expressing wild-type BRMS1. D: Expression of S237A mutant reverses BRMS1-mediated inhibition in cell migration (quantified in E).

One of the most accepted *in vitro* phenotypes associated with BRMS1 expression is the induction of anoikis cell death upon culture of cells under the anchorage-independent conditions [11]. Therefore, we then asked if the expression of S237A BRMS1 mutant had any effect on the induction of anoikis. As shown in Fig. 4A-B, upon expression of the wild-type BRMS1, there was a significant reduction in the overall number of cells remaining in culture after a 24-hr suspension culture. Moreover, we also detected a significant reduction in the number of BRMS1-expressing live cells under the same conditions. However, KPL4 cells expressing the S237A BRMS1 mutant did not exhibit a similar phenotype. Interestingly, we also found that anoikis conditions highly enhanced AMPK activity, as evidenced by the phosphorylation of ACC, one of the major AMPK substrates (Fig. 4C). However, activation of AMPK did not inhibit STAT3 phosphorylation that is associated with AMPK activation through pharmacologic means [12]. Since AMPK activating compounds, such as 2-DG and Metformin, are being tested in pre-clinical applications as potential anti-cancer drugs, in the future we plan to evaluate whether the S237A mutation in BRMS1 plays a role in the regulation of STAT3 signaling under those conditions.

Finally, we examined the effect of S237A BRMS1 mutation on the migratory ability of breast cancer cells. As shown in Fig. 4D (and quantified in Fig. 4E), expression of wild-type BRMS1 significantly inhibited the migration of both KPL4 and MDA-231 cells. Although KPL4 cells are poorly migratory, vector cells were able to close ~40% of the wound area within the 24-hrs, as compared to wild-type BRMS1-expressing cells that only closed about 25% of the wound. As with the earlier experiments, expression of the S237A BRMS1 mutant reversed BRMS1-mediated phenotype on the cell migration ability.

Based on all these data and previously published reports, we propose the following model for the effect of BRMS1 expression in breast cancer cells (Fig. 5): When BRMS1 is expressed, it is phosphorylated on S237, presumably by AMPK. Upon this phosphorylation, BRMS1 enhanced HDAC1/2 activity and promotes association of the mSin3A complex.

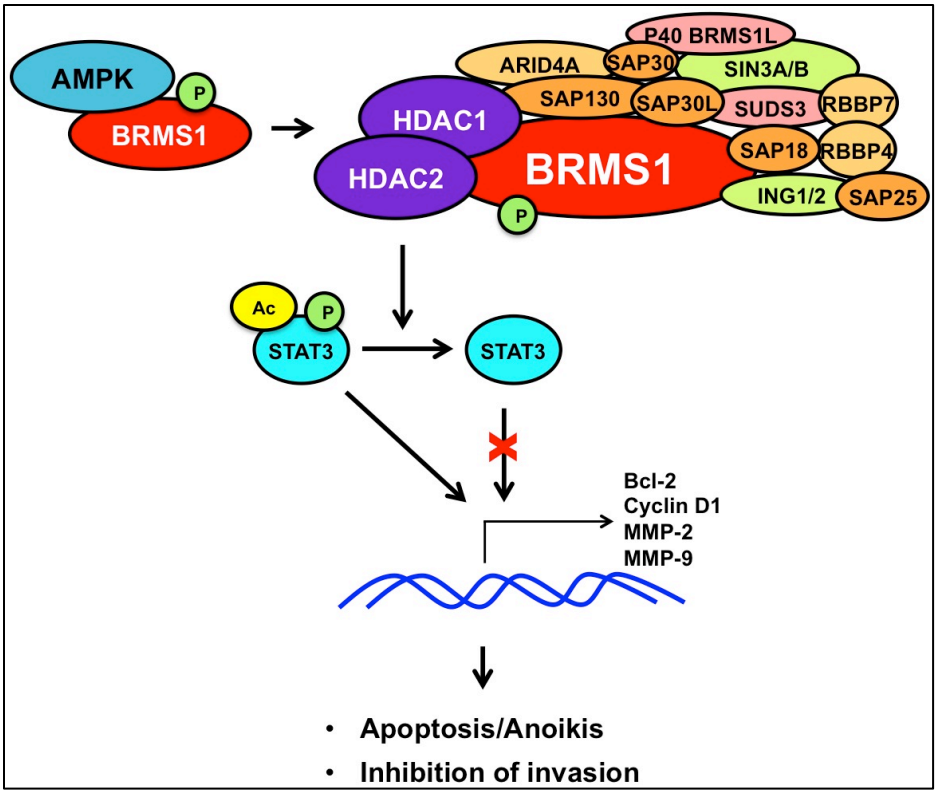

Then, HDAC1 activity leads to de-acetylation of STAT3, which in turn decreases its phosphorylation and inhibits the expression of the STAT3-driven genes, such as those responsible for cell survival and regulation of migration/invasion.

If these results hold true, they might begin to explain the seemingly discrepant results between BRMS1 expression and patient survival, where in some cases BRMS1 promotes better patient survival and in some cases it does not. Importantly, according to the TCGA tumor sequencing data, BRMS1 is frequently mutated, including on S237 that we identified to play an important role on BRMS1 exerting its anti-tumorigenic and anti-metastatic effects.

Figure 5. A-B: Proposed model of BRMS1 role in regulation of STAT3 signaling.

Task 2.5. Our findings describing the role of BRMS1 in cell adhesion and spreading were recently published in *Molecular Carcinogenesis* (see Appendix 2).

4. Key Research Accomplishments

4.1. Confirmed BRMS1 interaction with a kinase (AMPK) and a cytoplasmic protein implicated in cell motility (Filamin B).
4.2. Established a critical role for BRMS1 phosphorylation of S237.
4.3. Completed and published a paper describing the role of BRMS1 in regulation of cell adhesion and cell spreading.

5. Reportable outcomes

5.1. Khotskaya YB, Goverdhan A, Shen J, Ponz Sarvice M, Chang S-S, Hsu M-C, Wei Y, Xia W, Steeg P, Yu D, and Hung MC. (2013) S6K1 promotes invasiveness of breast cancer cells in a novel model of triple-negative breast cancer metastasis. Abstract for poster presentation at the AACR's The Translational Impact of Model Organisms in Cancer, San Diego, CA

5.2. Khotskaya YB, Beck BH, Hurst DR, Han Z, Xia W, Hung MC, and Welch DR. Expression of metastasis suppressor BRMS1 in breast cancer cells results in a marked delay in cellular adhesion to matrix. ***Mol Carcinog***. (2013)

5.3. Shen J, Xia W, Khotskaya YB, Huo L, Nakanishi K, Lim SO, Du Y, Wang Y, Chang WC, Chen CH, Hsu JL, Wu Y, Lam YC, James BP, Liu X, Liu CG, Patel DJ, Hung MC. EGFR modulates microRNA maturation in response to hypoxia through phosphorylation of AGO2. ***Nature*** (2013)

5.4. Saldana SM, Lee HH, Lowery FJ, Khotskaya YB, Xia W, Zhang C, Chang SS, Chou CK, Steeg PS, Yu D, Hung MC. Inhibition of type I insulin-like growth factor receptor signalin attenuates the development of breast cancer brain metastasis. **PLoS One** (2013)

6. Conclusion

6.1. BRMS1 interacts with and is phosphorylated by AMPK.
6.2. In KPL4 breast cancer cells, BRMS1 exhibits a single phosphorylated serine residue.
6.3. Mutation of that serine residue to non-phosphorylatable mimetic alanine abolishes BRMS1-mediated induction of anoikis and inhibition of cellular migration.

7. References

1. Hicks DG, Yoder BJ, Short S, Tarr S, Prescott N, et al. (2006) Loss of breast cancer metastasis suppressor 1 protein expression predicts reduced disease-free survival in subsets of breast cancer patients. Clin Cancer Res 12: 6702-6708.
2. Yamauchi H, Woodward WA, Valero V, Alvarez RH, Lucci A, et al. (2012) Inflammatory Breast Cancer: What We Know and What We Need to Learn. Oncologist 17: 891-899.
3. Kurebayashi J, Otsuki T, Tang CK, Kurosumi M, Yamamoto S, et al. (1999) Isolation and characterization of a new human breast cancer cell line, KPL-4, expressing the Erb B family receptors and interleukin-6. Br J Cancer 79: 707-717.
4. Meehan WJ, Samant RS, Hopper JE, Carrozza MJ, Shevde LA, et al. (2004) Breast cancer metastasis suppressor 1 (BRMS1) forms complexes with retinoblastoma-binding protein 1 (RBP1) and the mSin3 histone deacetylase complex and represses transcription. J Biol Chem 279: 1562-1569.
5. Hardie DG (2011) AMP-activated protein kinase: an energy sensor that regulates all aspects of cell function. Genes Dev 25: 1895-1908.
6. Neumann D, Woods A, Carling D, Wallimann T, Schlattner U (2003) Mammalian AMP-activated protein kinase: functional, heterotrimeric complexes by co-expression of subunits in Escherichia coli. Protein Expr Purif 30: 230-237.
7. Hardie DG, Alessi DR (2013) LKB1 and AMPK and the cancer-metabolism link - ten years after. BMC Biol 11: 36.
8. Moffat C, Ellen Harper M (2010) Metabolic functions of AMPK: aspects of structure and of natural mutations in the regulatory gamma subunits. IUBMB Life 62: 739-745.
9. Wang R, Cherukuri P, Luo J (2005) Activation of Stat3 sequence-specific DNA binding and transcription by p300/CREB-binding protein-mediated acetylation. J Biol Chem 280: 11528-11534.
10. Ray S, Lee C, Hou T, Boldogh I, Brasier AR (2008) Requirement of histone deacetylase1 (HDAC1) in signal transducer and activator of transcription 3 (STAT3) nucleocytoplasmic distribution. Nucleic Acids Res 36: 4510-4520.
11. Phadke PA, Vaidya KS, Nash KT, Hurst DR, Welch DR (2008) BRMS1 suppresses breast cancer experimental metastasis to multiple organs by inhibiting several steps of the metastatic process. Am J Pathol 172: 809-817.
12. Harada Y, Ishii I, Hatake K, Kasahara T (2012) Pyrvinium pamoate inhibits proliferation of myeloma/erythroleukemia cells by suppressing mitochondrial respiratory complex I and STAT3. Cancer Lett 319: 83-88.

Appendix 1 (Copy of Abstract accepted for presentation at the AACR's The Translational Impact of Model Organisms in Cancer, San Diego, CA, 2013)

S6K1 promotes invasiveness of breast cancer cells in a novel model of triple-negative breast cancer metastasis

Yekaterina B. Khotskaya, Aarthi Goverdhan, Jia Shen, Mariano Ponz Sarvice, Shih-Shin Chang, Ming-Chuan Hsu, Yongkun Wei, Weiya Xia, Patricia Steeg, Dihua Yu, and Mien-Chie Hung

Introduction:
Breast cancer is the second-leading cause of oncology-related death in US women. Despite extensive research, over 30% of breast cancer patients develop metastatic disease, and metastases account for majority of breast cancer-associated morbidity and mortality. Of all invasive breast cancers, patients with tumors lacking expression of the Estrogen and Progesterone hormone Receptors and Human Epidermal growth factor Receptor 2 have the poorest clinical prognosis. These triple-negative tumors (TNBC) represent an aggressive form of the disease that is marked by an early-onset metastasis, a high tumor recurrence rate, and a low overall survival during the first three years post-diagnosis. However, few TNBC mouse models of metastasis currently exist.

Results:
We noticed that a well-established MDA-MB-231 TNBC cell line produces rapid and extremely lytic bone lesions in lumbar, sacral and caudal vertebrae, and hind limbs in about 10% of animals injected intravenously. We biopsied one of these bone metastases and established a new metastatic MDA-MB-231-1566 cell line. Following an intravenous injection, MDA-MB-231-1566 cells produce early-onset metastasis to bone in up to 70% of animals with concurrent metastases to lungs, liver, and soft tissues. We demonstrate that 100% of animals injected with MDA-MB-231-1566 cells developed metastasis and had median survival of 60 days vs. 80 days in mice injected with the parental cell line. We also demonstrate that ribosomal protein S6 is highly phosphorylated on Ser235/236 in metastatic TNBC tumors, and that this phosphorylation is indicative of upstream S6 kinase (S6K) activity. Lastly, we provide evidence that targeting S6K with a highly specific inhibitor, PF-4708671, at sub-lethal doses inhibits cell migration without inducing cell death, and thus may provide a potent anti-metastatic adjuvant therapy approach.

Conclusion:
We established a new model of rapid TNBC metastases to multiple organs following a simple intravenous injection. We believe this model provides a valuable tool for screening new therapeutics aimed to stop growth of metastases.

Appendix 2 (Copy of our paper in *Molecular Carcinogenesis*)

Expression of Metastasis Suppressor BRMS1 in Breast Cancer Cells Results in a Marked Delay in Cellular Adhesion to Matrix

Yekaterina B. Khotskaya,[1,2] Benjamin H. Beck,[1] Douglas R. Hurst,[1,3] Zhenbo Han,[2] Weiya Xia,[2] Mien-Chie Hung,[2,4,5], and Danny R. Welch[1,3,6]***

[1]*Department of Pathology, University of Alabama at Birmingham, Birmingham, Alabama*
[2]*Department of Molecular and Cellular Oncology, The University of Texas MD Anderson Cancer Center, Houston, Texas*
[3]*Comprehensive Cancer Center, University of Alabama at Birmingham, Birmingham, Alabama*
[4]*Department of Biotechnology, Asia University, Taichung, Taiwan*
[5]*Graduate Institute of Cancer Biology and Center for Molecular Medicine, China Medical University, Taichung, Taiwan*
[6]*Department of Cancer Biology and the Kansas University Cancer Center, Kansas University Medical Center, Kansas City, Kansas*

Metastatic dissemination is a multi-step process that depends on cancer cells' ability to respond to microenvironmental cues by adapting adhesion abilities and undergoing cytoskeletal rearrangement. Breast Cancer Metastasis Suppressor 1 (BRMS1) affects several steps of the metastatic cascade: it decreases survival in circulation, increases susceptibility to anoikis, and reduces capacity to colonize secondary organs. In this report, BRMS1 expression is shown to not significantly alter expression levels of integrin monomers, while time-lapse and confocal microscopy revealed that BRMS1-expressing cells exhibited reduced activation of both β1 integrin and focal adhesion kinase, and decreased localization of these molecules to sites of focal adhesions. Short-term plating of BRMS1-expressing cells onto collagen or fibronectin markedly decreased cytoskeletal reorganization and formation of cellular adhesion projections. Under 3D culture conditions, BRMS1-expressing cells remained rounded and failed to reorganize their cytoskeleton and form invasive colonies. Taken together, BRMS1-expressing breast cancer cells are greatly attenuated in their ability to respond to microenvironment changes.

Key words: BRMS1; metastasis; adhesion; integrins; CTC

INTRODUCTION

The metastatic cascade is a multi-step and highly inefficient process [1–4]. As cancer cells gain the ability to metastasize, they must complete a series of sequential events: dissociate from primary tumor, intravasate into lymphatic or systemic circulation, survive shear stress while in circulation, extravasate into and proliferate at a secondary site [4–9]. Consequently, interfering with any of these steps would preclude development of overt metastases [10–12].

A cancer cell's behavior can be affected at individual steps of the metastatic cascade by the microenvironment in which the tumor finds itself. This cell/microenvironment interaction and the cell's ability to relay signals from the surroundings affect it's ability to proliferate, migrate, adhere and overcome cellular senescence [7,13–17]. Cancer cell/extracellular matrix (ECM) interactions can be studied using relatively simple in vitro models [18] or complex in vivo evaluations [19–23]. Nonetheless, the majority of

Abbreviations: ECM, extracellular matrix; FAK, focal adhesion kinase; ILK, integrin linked kinase; MRTF, myocardin-related transcription factor; SRF, serum response factor; BRMS1, breast cancer metastasis suppressor 1; CTC, circulating tumor cells; DTC, disseminated tumor cells

Contract grant sponsor: University of Alabama at Birmingham Center for Metabolic Bone Diseases; Contract grant number: AR047512-08; Contract grant sponsor: Department of Defense (DOD) Congressionally Directed Medical Research Breast Cancer Research Program; Contract grant number: W81XWH-10-1-0749; Contract grant sponsor: American Cancer Society; Contract grant number: RSG-11-259-01-CSM; Contract grant sponsor: National Foundation for Cancer Research Center for Metastasis Research; Contract grant sponsor: National Institute of Health; Contract grant number: RO1-CA87728, RO1-CA134981, P30-CA168524; Contract grant sponsor: Susan G. Komen for the Cure; Contract grant number: SAC 11037; Contract grant sponsor: The University of Texas MD Anderson-China Medical University and Hospital Sister Institution Fund; Contract grant sponsor: MD Anderson Cancer Center; Contract grant number: CA16672; Contract grant sponsor: MD Anderson Center for Biological Pathways; Contract grant sponsor: National Breast Cancer Foundation, Inc.; Contract grant sponsor: Program for Stem Cell and Regenerative Medicine Frontier Research (Taiwan); Contract grant number: NSC101-2321-B-039-001; Contract grant sponsor: International Research-Intensive Centers of Excellence in Taiwan; Contract grant number: NSC102-2911-I-002-303; Contract grant sponsor: Cancer Research Center of Excellence (Taiwan); Contract grant number: DOH102-TD-C-111-005

*Correspondence to: Department of Cancer Biology, The Kansas University Medical Center, 3901 Rainbow Boulevard, Kansas City, KS 66160.

**Correspondence to: Department of Molecular and Cellular Oncology, The University of Texas MD Anderson Cancer Center, Box 108, 1515 Holcombe Boulevard, Houston, TX 77030.

Received 6 March 2013; Revised 22 May 2013; Accepted 17 June 2013

DOI 10.1002/mc.22068

Published online in Wiley Online Library (wileyonlinelibrary.com).

studies have focused on tumor cells while they are still associated with the primary tumor mass or after they have extravasated [24–27]. However, with advances in ability to detect circulating tumor cells and their strong association with poorer patient prognosis [28–30], it is becoming necessary to pay more attention to understanding what is taking place "in-between", that is, adhesion and survival while tumor cells are still in the circulation, both to find novel therapeutic targets and to establish possible biomarkers and prognostic markers.

Adhesion and consequent anoikis protection are regulated, by and large, through the interaction of integrins and their appropriate extracellular substrates. Integrins are cell surface heterodimers that exist in two conformations: "inactive" bent conformation, and "active" upright conformation [31,32]. The shift in conformations is initiated upon formation of a focal adhesion complex, followed by phosphorylation of focal adhesion kinase (FAK), activation of integrin linked kinase (ILK) and downstream actin and microtubular cytoskeleton remodeling. Actin cytoskeleton remodeling (reviewed in [33,34]) initiates further morphologic and transcriptional changes: globular actin levels decrease during actin filament polymerization, stimulating translocation of myocardin-related transcription factor (MRTF, also called MAL) into the nucleus, where it binds to serum response factor (SRF) and together, they initiate transcription of many actin cytoskeleton genes and genes regulating focal adhesion assembly, such as $\alpha 5$ integrin, Tenascin C, Talin-1, Profilin 1, and Actinin [35].

Intravital microscopy had shown that a metastatic cancer cell spends in the range of few seconds to few minutes in circulation [36–38]. At the time of intravasation, tumor cells undergo a morphologic change, from initially rounded and detached to loosely, and

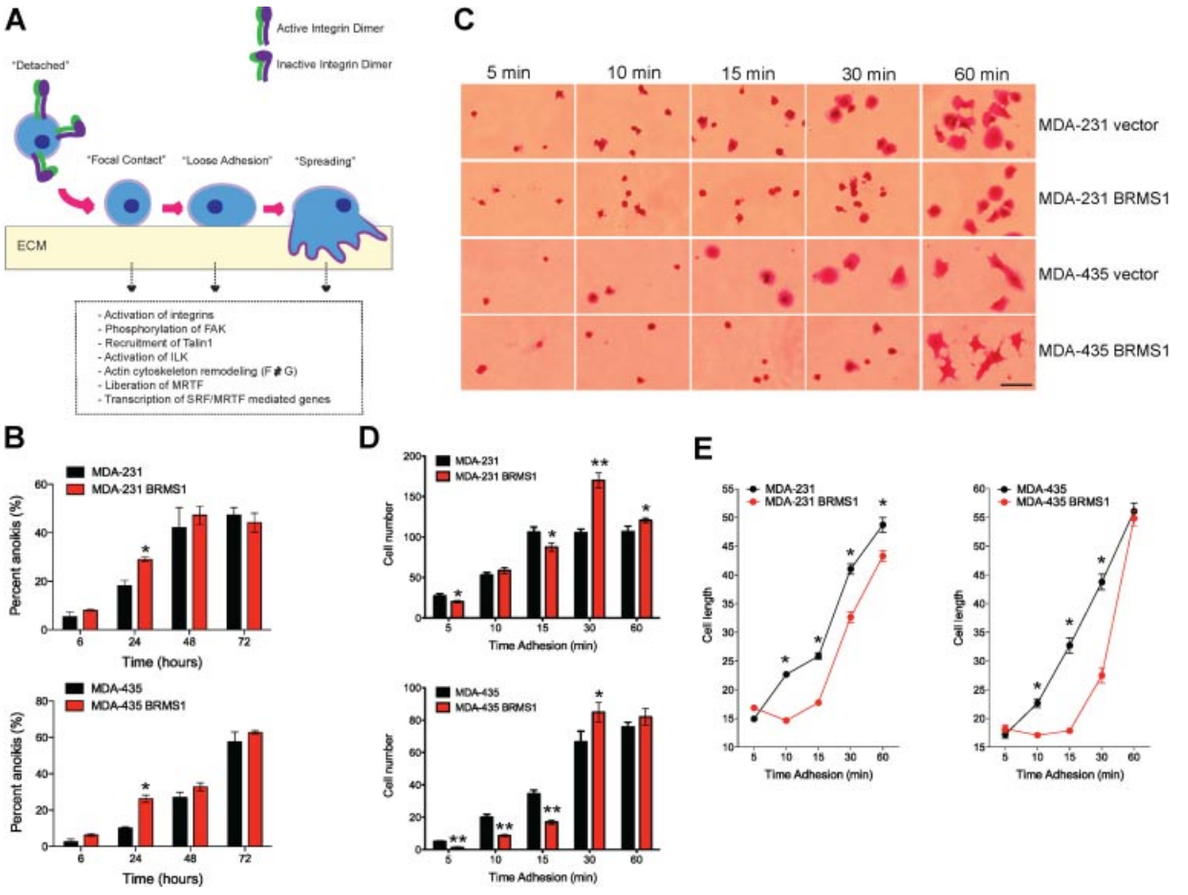

Figure 1. BRMS1 delays adhesion of MDA-231 and MDA-435 breast cancer cells. (A) Model of adhesion cascade as examined in this manuscript. (B) Vector control and BRMS1-expressing cells were plated onto ultra-low adhesion plate in complete media and maintained in a suspension culture for 72 h. At times noted, anoikis was assessed by direct counts of live and dead cells utilizing trypan blue. (C) Vector control and BRMS1-expressing breast cancer cells were plated onto optical plates precoated with whole FBS and allowed to adhere for time indicated, at which point cells were fixed and stained with crystal violet. Representative images for times 5, 10, 15, 30, and 60 min are shown. Scale bar = 20 μm. (D) Quantification of adherent cell numbers. Data are representative of triplicate experiments and are expressed as mean ± SEM ($^{*}P < 0.05$, $^{**}P < 0.001$). (E) Quantification of cell length at times indicated, as measure of cell spreading. Cell length was measured in pixels in ImageJ. Data are representative of triplicate experiments and are expressed as mean ± SEM ($^{*}P < 0.00001$).

eventually, more strongly, adherent [39]. During circulation, the cell must adhere to an appropriate matrix or endothelial cells in order to avoid anoikis (Figure 1A) [40,41]. Furthermore, cancer cells frequently masquerade as normal cells, including their ability to act similar to leukocytes homing towards sights of inflammation [42]. Expanding on this idea, we hypothesized that disseminating cancer cells may, similar to leukocytes, utilize the process of rolling adhesion to slow down and initiate extravasation. Leukocytes slow down first by tethering to and rolling on endothelial cells via clustering of cell surface selectins and integrins to form "docking structures" [43–45]. Upon loose adhesion, leukocytes then initiate strong contact with ECM and endothelial cells, followed by rapid cytoskeletal rearrangement, which allows diapedesis into appropriate tissues [46–50]. Therefore, one of the objectives of the current study was to address the hypothesis of leukocyte-like breast cancer cell behavior by utilizing an in vitro adhesion model representative of adhesion in vivo. For these purposes, we chose to use a well-described model of pairs of highly metastatic and metastases suppressed MDA-MB-231 (MDA-231) and MDA-MB-435 (MDA-435) breast cancer cells with (metastasis suppressed) or without (metastatic) ectopic expression of breast cancer metastasis suppressor 1 (BRMS1). While the origin of MDA-435 cell line is somewhat controversial, several recent reports shed more light onto its genesis and convincingly show that these cells are capable of tumor formation and metastases from the mammary fat pad of immunocompromised mice, express epithelial cell markers, and make milk proteins and lipids [51,52].

BRMS1 is a metastasis suppressor that, by definition, suppresses metastasis without significantly affecting the growth of a primary tumor [4,53]. Mechanistically, BRMS1-expressing cells exhibit decreased survival in circulation [54] and are less capable of seeding secondary sites, which is partially attributed to BRMS1-enhanced anoikis [55]. However, precise mechanisms regulating anoikis in BRMS1-expressing cells are unclear. Further, BRMS1-expressing cells that seed secondary sites remain there as single cells or in small colonies, but are unable to form overt metastases [55]. Interestingly, initial steps of the metastatic cascade, such as local invasion and intravasation, appear to be unaffected by BRMS1 expression [56,57]. We therefore hypothesized that BRMS1 expression alters cancer cells' ability to properly interpret and respond to extracellular signals after cells dissociated from the primary tumor, both during transport by systemic circulation and upon reaching secondary sites.

In this study, we utilized time-lapse and confocal microscopy to evaluate changes in adhesion complex assembly and organization and cell spreading brought about by BRMS1 expression, especially in response to extracellular composition. Short-term cell/ECM interactions bring about morphologic changes, as well as the associated signaling transduction changes, which correspond to BRMS1 expression. Consequently, MDA-231 and MDA-435 cells expressing BRMS1 are less capable of interacting with and invading into the surrounding matrix. Taken together, these results suggest that BRMS1 expression assessed in circulating or disseminated tumor cells, that is, more than in primary tumor cells, may be useful for predicting the possibility of metastatic relapse.

RESULTS

BRMS1 Delays Adhesion of MDA-231 and MDA-435 Breast Cancer Cells

BRMS1 expression in breast cancer cells exhibits no effect on cell proliferation in vitro (Supplementary Figure 1). At the same time, earlier studies characterizing BRMS1 effect on cell adhesion showed that BRMS1 marginally affected cell adhesion to matrix [57]. BRMS1 expression did, however, significantly promote anoikis of breast cancer cells [55], which we also confirmed in the present study (Figure 1B). To examine if earlier steps of adhesion, such as cell attachment to matrix and cell spreading, might attribute for BRMS1-associated anoikis, we gently detached vector or BRMS1-expressing MDA-231 and MDA-435 cells with EDTA as to not cleave any membrane receptors. Cells were then plated onto optical plates precoated with FBS representing matrix milieu and imaged by time-lapse microscopy for 1 h or fixed and stained with crystal violet at times indicated. As shown in Figure 1C and quantified in Figure 1D and E, in both cell lines BRMS1 expression delayed morphologic progression from round to spread (10, 15, and 30 min postplating). However, by 1 h postplating, vector control and BRMS1-expressing cells were similar in appearance and behavior, both morphologically and based on total number adherent cells (Figure 1D and Supplementary Movies 1–4).

BRMS1 Expression Has Little Effect on Integrin Expression, but Reduces Activated β1 Integrin Localization to Adhesion-Associated Cellular Protrusions

Since many adhesion events are mediated through modulation of expression and activity of integrins, we then asked whether BRMS1-associated adhesion changes were due to downregulation of integrin expression. We first confirmed BRMS1 expression in MDA-231 and MDA-435 cells we previously established and characterized (Figure 2A and Supplementary Figure 1B), and then assayed their whole cell lysates for expression of several integrin monomers and observed only a slight reduction in α5 integrin levels (Figure 2B). We then performed confocal microscopy 15 and 30 min after plating cells onto FBS-coated slides to examine whether there were changes in activation status and cellular localization

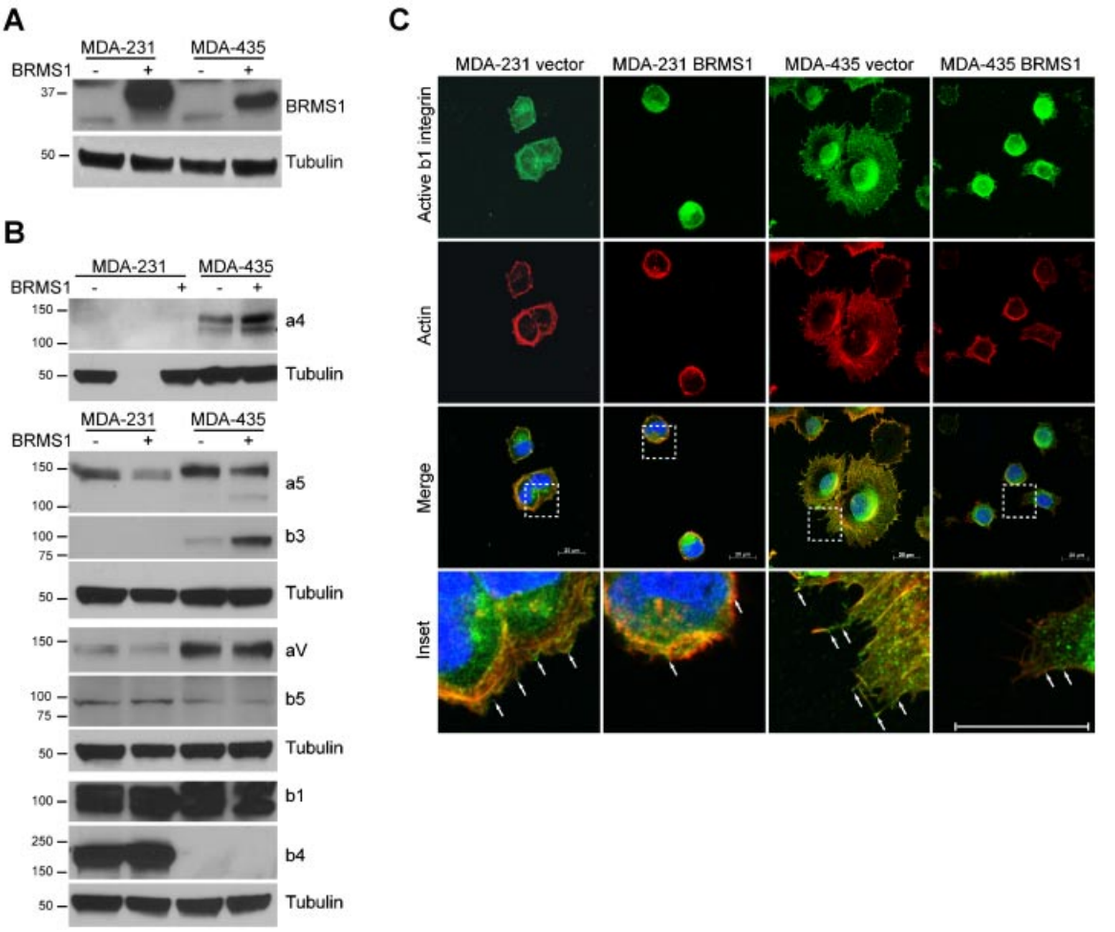

Figure 2. BRMS1 does not significantly affect expression of integrin monomers, but reduces localization of activated β1 integrin to adhesion-associated cellular protrusions. (A) Vector control and BRMS1-expressing breast cancer cells grown under normal culture conditions were examined by Western blotting for expression of BRMS1. (B) Vector control and BRMS1-expressing breast cancer cells grown under normal culture conditions were examined by Western blotting for expression of integrin monomers indicated. (C) Vector control and BRMS1-expressing cells were plated onto chamber slides precoated with FBS and allowed to adhere for 15 min. Fixed cells were stained for actin (red) and activated β1 integrin (green). Nuclei were stained with DAPI (blue) for reference. Arrows indicate active β1 integrin foci localized to outer-most cell membrane. Scale bar = 20 μm.

of β1 integrin, a binding partner for many α subunits and a known player in metastases (Figure 2C; Supplementary Figure 2). At both times, cells transfected with empty vector exhibited thicker actin cytoskeleton rings (red fluorescence signal) and appeared more spread, whereas BRMS1-expressing cells remained rounded and exhibited highly condensed cytoplasm. Moreover, activated β1 integrin (green fluorescence signal) localized to the outer membrane edge of cells where focal adhesions are found, also co-localizing with the actin rings. These data suggest that BRMS1 may impede appropriate localization of activated integrins to the focal adhesion complexes, thereby altering adhesion and cell spreading. Alternatively, BRMS1 may delay clustering of integrin heterodimers already present at the plasma membrane, which would lead to a delay in adhesion. Lastly, BRMS1 may directly affect endoplasmic spreading, which was recently shown to be regulated through cooperation of cellular adhesions and intermediate filaments [58].

BRMS1 Decreases Focal Adhesion Complex Assembly

To determine whether other components of the focal adhesion complex were affected by BRMS1 expression, we first performed short-term (15 min postplating) adhesion assay followed by confocal microscopy. We used distribution of FAK phosphorylated on tyrosine 397 as a marker of focal adhesion complex. As shown in Figure 3A, and consistent with the findings described above, BRMS1-expressing cells did not spread as well as the vector control cells, defined by actin cytoskeleton reorganization. Further, fewer BRMS1-expressing cells exhibited

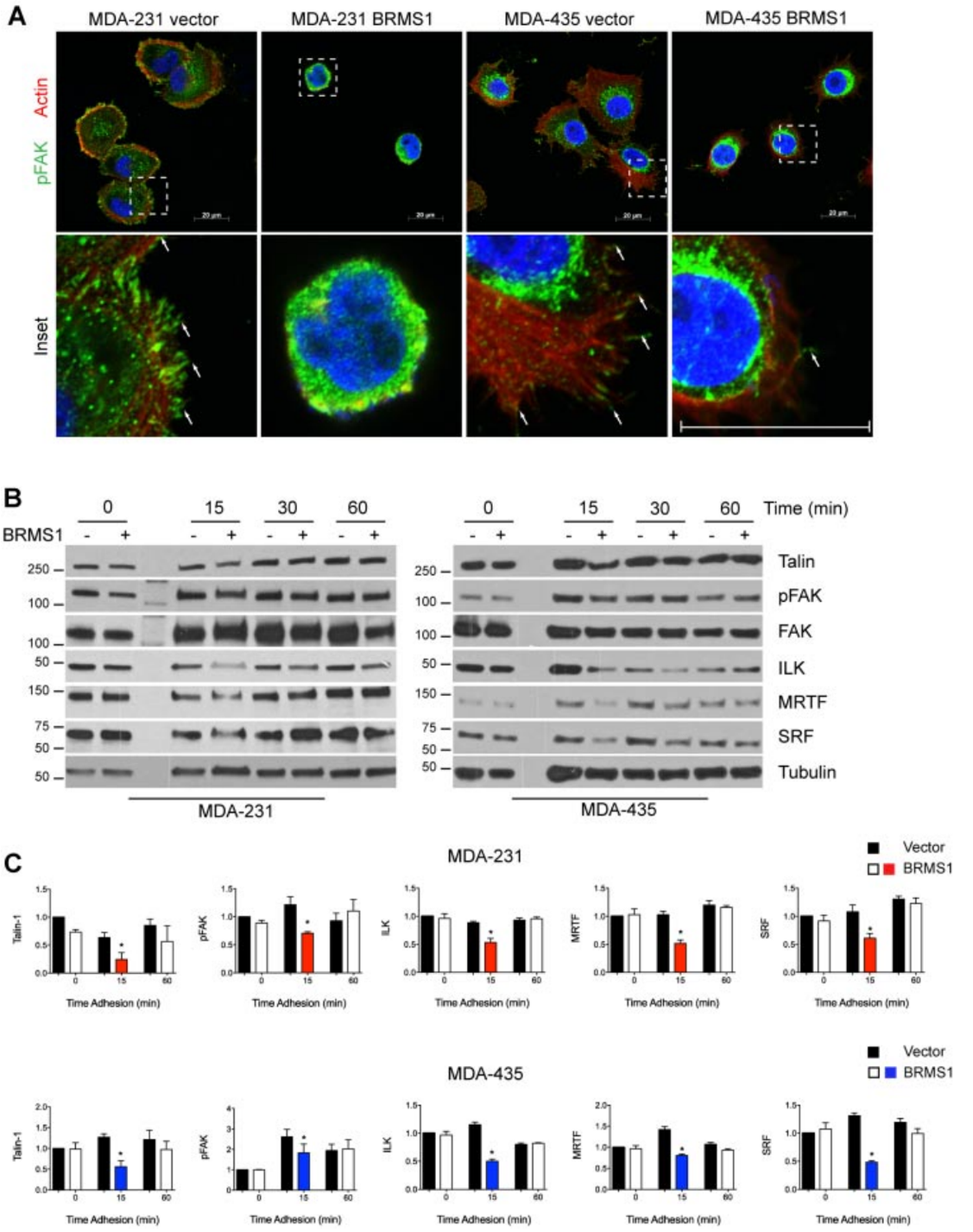

Figure 3. BRMS1 decreases focal adhesion complex assembly. (A) Vector control and BRMS1-expressing cells were plated onto chamber slides precoated with whole FBS and allowed to adhere for 30 min. Fixed cells were stained for actin (red) and pFAK (green) to indicate focal adhesions. Nuclei were stained with DAPI (blue) for reference. Arrows indicate pFAK foci, indicative of focal adhesions, localized to outer-most cell membrane. Scale bar = 20 μm. (B) Vector and BRMS1-expressing cells were plated onto plates precoated with FBS and lysed at times indicated. Whole cell lysates were assayed by Western blotting for levels of markers of focal adhesions or those indicative of actin remodeling cytodynamics. (C) Bar graphs depict Western blot quantitations at various times. Data are representative of triplicate experiments and are expressed as mean ± SEM. $^{*}P < 0.05$.

pFAK localized to the outer-most cell surface in regions where focal adhesions would be found, further indicating alterations in adhesion. Interestingly, BRMS1-expressing cells exhibited a strong cytoplasmic and perinuclear pFAK (Figure 3A) and activated β1 integrin (Figure 2C) localization, suggesting that BRMS1 may accelerate recycling of cytoplasmic receptors, such as integrins and other member of the focal adhesion complex, or prevent their outward trafficking towards plasma membrane, thereby reducing their membranous localization.

To confirm the microscopy data, adhesion was measured over time concomitant with analysis of adhesion protein quantification using immunoblot. Consistent with previously published data that BRMS1 did not affect adhesion to ECM at 1 h postplating [57], there was little difference in expression of focal adhesion markers at 1-hour postplating (Figure 3B and C). However, at 15 min (Figure 3B and C), there was a simultaneous reduction in expression of all focal adhesion-associated markers, such as Talin, pFAK, and ILK, suggesting that expression of BRMS1 affected the earliest events involved in cell adhesion.

Confocal microscopy revealed a delay in proper reorganization of actin cytoskeleton in response to matrix stimulation conferred by BRMS1. Therefore, we examined expression levels of two markers of actin cytoskeleton remodeling, MRTF and SRF. Levels of MRTF and SRF were significantly reduced 15 min postplating of cells (Figure 3C), but they leveled out by 30 min postplating, again suggesting that BRMS1 affects kinetics of cellular adhesion.

To address whether adhesion changes were dependent upon variations amongst ECM components by species [59], experiments were done utilizing matrix components of human origin. We also elected to look at extracellular matrices that were relevant to in vivo progression of breast cancer: collagen IV, a major constituent of tumor basement membrane and lung microenvironment; collagen I, a main extracellular component of bone microenvironment; and soluble fibronectin, a key protein component of human plasma. In general, all cancer cells tested took longer to adhere to collagens and fibronectin in the absence of serum (data not shown). Therefore, we only evaluated adhesion-related signaling events at 30 and 60 min postplating. As shown in Figure 4, there was a substantial decrease in expression of all focal adhesion and actin cytoskeleton remodeling-associated proteins at 30 min postplating. Regardless of substrate, BRMS1-expressing cells exhibited reduced cell spreading, formation of focal adhesion complexes, reduced membrane localization of pFAK and activated β1 integrin (Supplementary Figures 3 and 4). Together, these findings indicate that BRMS1 delayed adhesion independent of the substrate. Consequently, these findings may explain reduced survival of BRMS1-expressing cells in circulation, which would contribute to their inability to form overt metastases.

BRMS1 Expression Impairs Cell Invasion in 3D Cultures

As evidenced by Supplementary Movies 5–8, within several hours postplating onto collagen I as a 3D culture, vector control cells began to "probe" their surrounding matrix by extending long, dynamic cellular protrusions. Conversely, BRMS1-expressing cells formed few visible protrusions and stayed comparatively stationary. Interestingly, formation of these cellular protrusions in vector cells occurred in the presence or absence of serum, while even in the presence of serum BRMS1-expressing cells were unable to invade into the matrix (Figure 5A). These data suggest that even upon cellular stress, such as low nutrient conditions, BRMS1-expressing cells were unable to override their inability to interact with the surrounding matrix. If allowed to grow under 3D culture conditions, vector control cells formed large invasive colonies by 7–10 d. However, BRMS1-expressing cells formed smaller and low invasive colonies, albeit the overall number of colonies formed by vector and BRMS1-expressing cell lines was similar (Figure 5B)—MDA-231-vector: 192.5 $\pm$ 40.3 vs. MDA-231-BRMS1: 185.5 $\pm$ 17.7; MDA-435-vector: 159.5 $\pm$ 6.4 vs. MDA-435-BRMS1: 191.5 $\pm$ 10.6 (not statistically significant). Mechanistically, continuous culture of BRMS1-expressing cells in 3D collagen I led to a profound inhibition of Talin-1, pFAK, ILK, and MRTF, as compared to vector control cells (Figure 5C). At the same time, continuous culture of cells under 2D culture conditions on plastic did not yield same results (Figure 5C). Interestingly, there were no appreciative differences in activation of any growth-associated signaling cascades, that is, AKT, ERK, Jun, or apoptosis-related signaling cascade between vector and BRMS1-expressing cells (data not shown).

To confirm lack of invasion by BRMS1-expressing cells under 3D conditions, we also performed a 3D culture assay utilizing Matrigel, which combines several types of ECM and growth factors. As shown in Figure 6A, BRMS1-expressing cells formed poorly invasive colonies when compared to vector-only cells. When we quantified invasive colonies, vector-only cells were significantly more invasive, as compared to BRMS1-expreesing cells (Figure 6B). As with Collagen I 3D cultures, the overall number of colonies formed by both cell types was similar (Figure 6B), as was their size (Figure 6C), suggesting that BRMS1-expressing breast cancer cells can proliferate, but not invade, when cultured under 3D conditions. Lastly, using shRNA, we partially knocked down BRMS1 expression in MDA-231 cells expressing exogenous BRMS1 (Figure 6D). Even this partial (30% and 50%) knockdown reversed BRMS1-mediated inhibition of invasion in 3D culture (Figure 6E) and adhesion to FBS-coated plates under 2D conditions (Figure 6F).

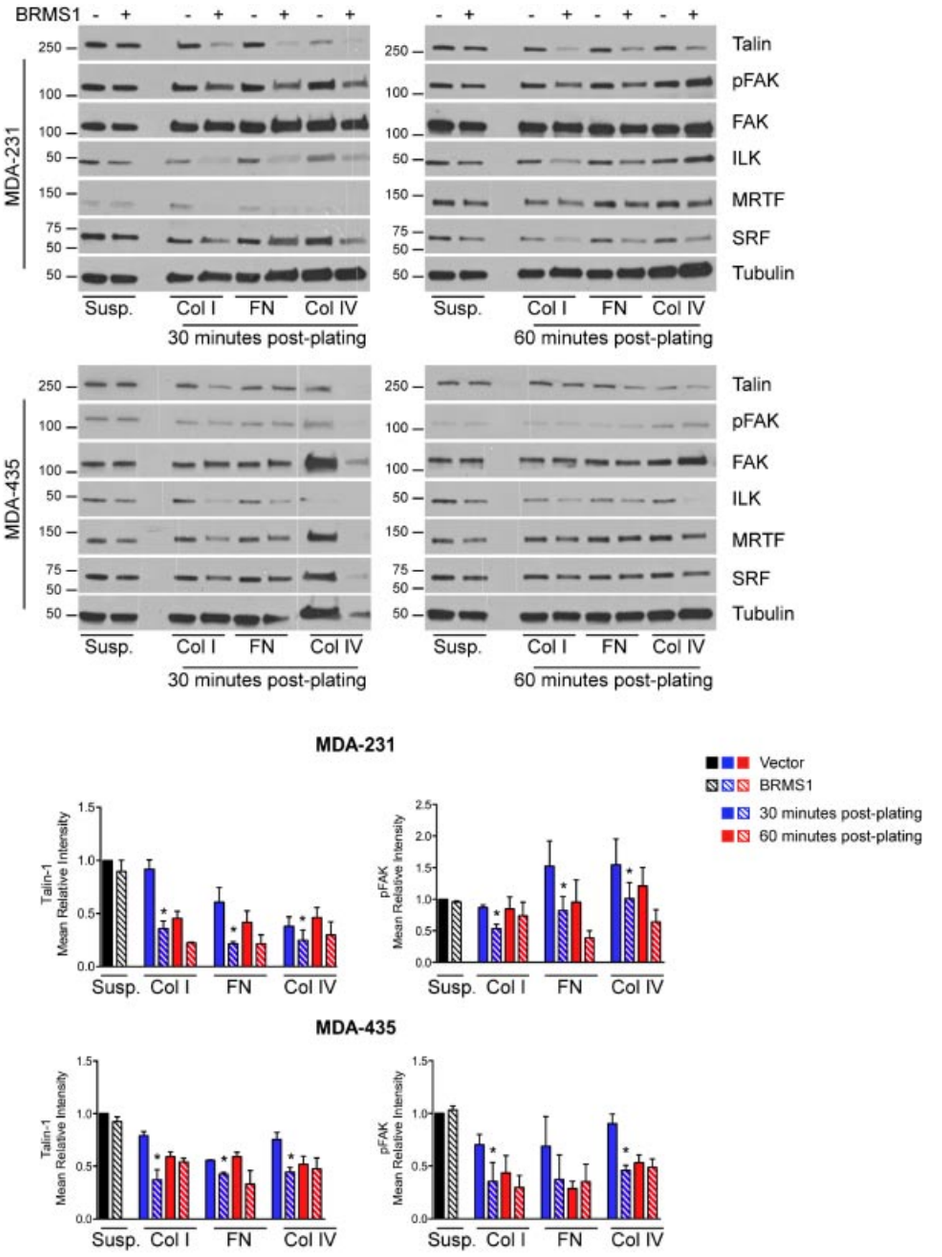

Figure 4. BRMS1 reduces adhesion of breast cancer cells to collagen I, collagen IV, and fibronectin. Vector and BRMS1-expressing cells were plated onto plates precoated with collagen I, collagen IV, or fibronectin and lysed at times indicated. Cells lysates were assayed by Western blotting for levels of markers of focal adhesions or indicative of actin remodeling cytodynamics. Bar graphs depict Western blot quantitation of Talin and pFAK levels at various times. Data representative of triplicate experiments and are expressed as mean ± SEM. $^{*}P < 0.05$.

Data presented in this manuscript show that BRMS1 somehow affects adhesion, and consequently, invasion of breast cancer cells. However, the question remains: how could a protein whose only known functions described thus far are restricted to the nucleus, be responsible for cytoskeletal modulation? We hypothesize that BRMS1 may, in fact, possess a yet-undefined cytoplasmic function. It had been shown previously that BRMS1 could be localized to the cytoplasm of breast cancer patients' tumors (Figure 7A and Ref. [60]). Upon examination of BRMS1-expressing cells used in this study, we also observed cytoplasmic localization of BRMS1 by both confocal analysis (Figure 7B) and Western blotting (Figure 7C). Taking into account previous reports of BRMS1 association with well-defined cytoplasmic

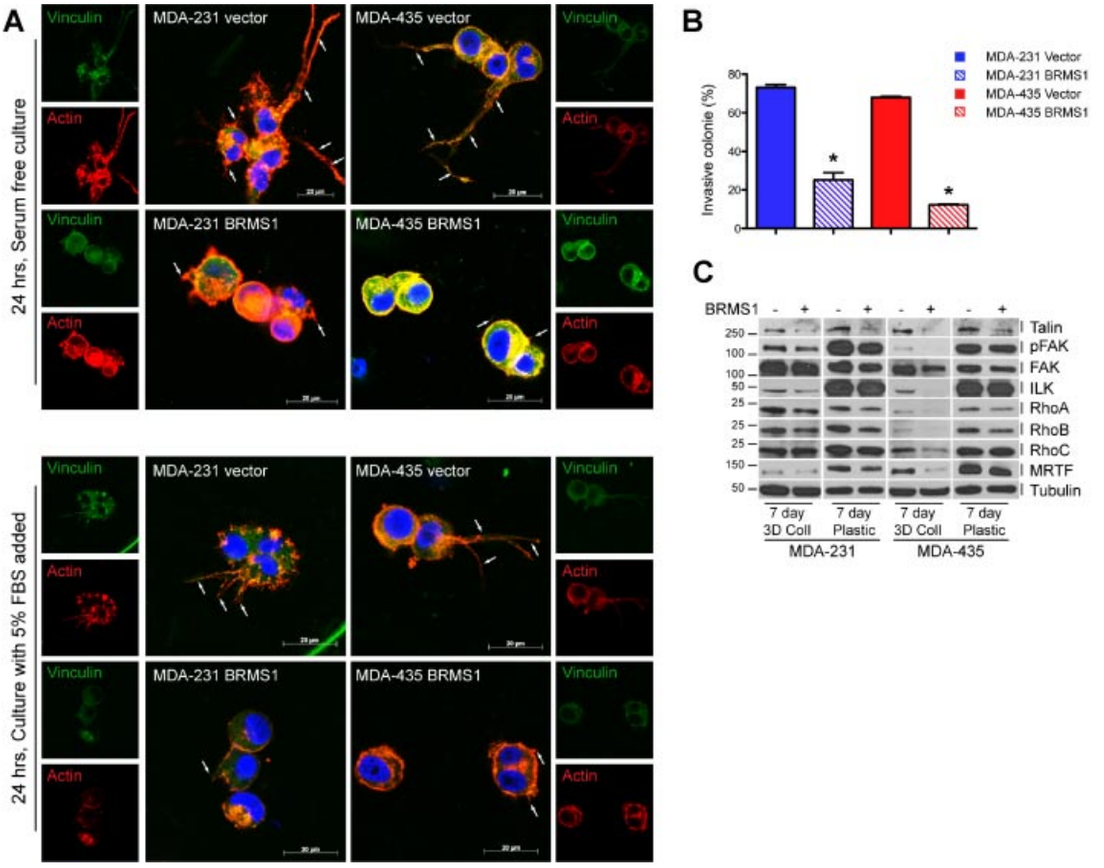

Figure 5. Expression of BRMS1 results in formation of smaller, less invasive colonies compared to vector control cells when grown in 3D collagen I culture. (A) Vector and BRMS1-expressing cells were plated in 3D collagen I for 24 h in growth media with or without FBS. After 24 h, cells were fixed and stained within gels, so not to disrupt cellular morphology, using vinculin to indicate focal adhesions (green) and actin (red) to visualize cytoskeleton. Nuclei were stained with DAPI (blue) for reference. Arrows point to cellular projections invading into the gels. Images are representative of triplicate experiments. Scale bar = 20 μm. (B) Cells plated in 3D collagen I were allowed to grow into colonies for 7–10 d in growth media supplemented with FBS, at which time gels were photographed and colonies counted. At least five different non-overlapping areas of the gel were examined at low magnification and at least 150 colonies counted per view area. Data shown are mean ± SEM. $^{*}P < 0.05$. (C) Cells grown in 3D collagen I culture or on plastic culture plates under 2D conditions (without re-plating) were lysed and lysates assayed by Western blotting for expression of focal adhesion or cytoskeletal remodeling proteins.

proteins known to regulate cytoskeletal rearrangement, such as HDAC6 [61] and smoothelin [62], it is possible that the events described in this manuscript occur through a direct interaction between BRMS1 and the cytoskeleton. This hypothesis is further confirmed by our recent observation of a direct interaction between BRMS1 and Filamin B, an actin cytoskeleton cross-linking protein (Khotskaya and Hung, unpublished data). Our future studies will aim at further dissecting BRMS1 functions, including those it may play in the cytoplasm.

DISCUSSION

Adhesion of cells to matrix is a major step that determines the success or failure of the metastatic cascade at every step. By carefully examining morphology and adhesion over a range of times, parameters that impact metastatic efficiency could be measured. Data confirm that the process of adhesion in vivo is dynamic, necessitating careful attention to adhesion kinetics. Specifically, one must ask: are cells that have adhered fully within 3–4 h after plating to static two-dimensional matrices representative of those extracted from a cancer patient, where cells must survive under shear, low oxygen and in the presence of immune cells? We suggest not. The current body of knowledge predicts that differences in adhesion (i.e., degree and pattern of spreading, as well as strength of adhesion) contribute to a cell's metastatic ability. As such, it is essential to use assays that address the "how" of adhesion: is the cell strongly attached (i.e., fully spread)? Is a cell rounded or weakly adherent? In this report, we utilized a combination of assays in order to determine "why" BRMS1-expressing cells do not survive as efficiently in circulation. Concurrently, the assays began to address how BRMS1 expression affects cell/matrix interactions.

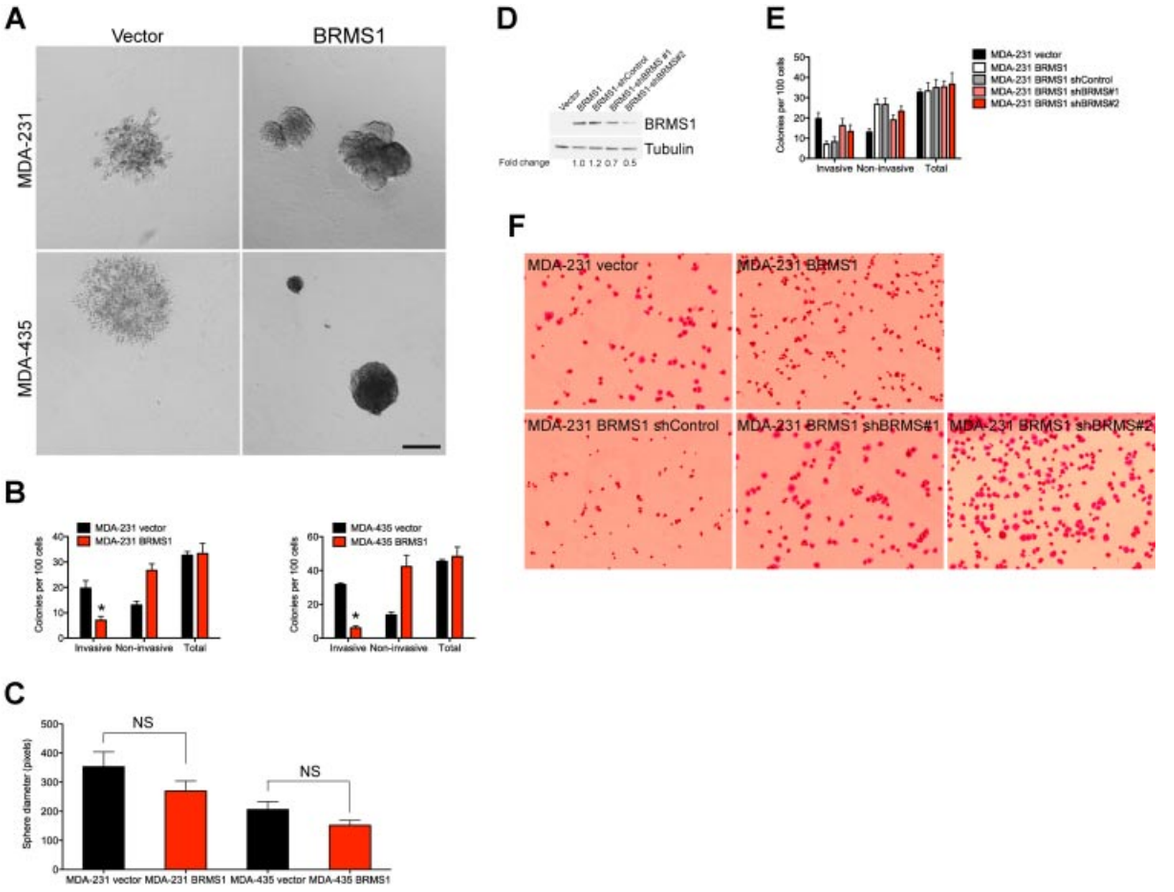

Figure 6. BRMS1 diminishes invasion of breast cancer cells in 3D matrigel cultures. (A) Cells plated in 3D Matrigel were allowed to grow into colonies for 12 d in growth media supplemented with FBS. Gels were photographed and colonies counted on day 12 to assess invasion. Images are representative of triplicate experiments. Scale bar = 200 μm. (B) Total number of colonies, number of invasive and non-invasive colonies was counted. Data shown are mean ± SEM. $^*P < 0.05$ (C) Colony size was measured in pixels using ImageJ. At least three fields per well of an experiment performed in triplicate were analyzed. Data shown are mean ± SEM. NS, no statistically significant difference. (D) BRMS1 expression was knocked down with two different shRNA clones. Cell lysates were collected and BRMS1 expression analyzed by Western blot. Fold change in BRMS1 expression was analyzed through ImageJ densitometry. (E) Ability of BRMS1-knockdown cells to invade into 3D matrigel was analyzed. Experiment was done at the same time as data shown in panel A, and vector control and BRMS1-expressing cells used for comparison. (F) Vector, BRMS1-expressing, and BRMS1-knockdown cells were plated onto FBS-coated plates and allowed to adhere for 30 min. Cells were fixed and stained with crystal violet for visualization.

Although it is firmly established that BRMS1 strongly suppresses metastases and that the biological effects are presumably through its effects on chromatin structure [63], the precise interconnection between these independent observations have not yet been determined. It has been described that BRMS1 expression significantly reduces survival of breast cancer cells in systemic circulation of immunocompromised mice [54,55]. Moreover, BRMS1 upregulates expression of pro-apoptotic genes associated with cells' inability to adhere, therefore inducing anoikis [55]. Consistent with data from Heyder et al. [64], time-lapse microscopy showed that vector control cells attach to matrix rapidly and almost immediately begin to spread in both 2D and 3D culture assays. In contrast, BRMS1-expressing cells remain rounded and weakly attached. Similarly, Krishnan et al., using a 3D bioreactor containing bone cells and breast carcinoma cells (±BRMS1 expression), showed that metastatic cells organized into invasive chords. In contrast, BRMS1-expressing cells were only loosely adherent [65]. If one couples those observations, they highlight that static measurement of adhesion events could miss critical parameters that contribute to invasion and metastasis. One must fully consider spatial and temporal regulation of adhesive molecules and the signaling through them. Since pFAK and activated β1 integrin have been shown to initiate adhesion by assembling focal adhesions and their deregulation leads to changes in anchorage-independent growth, our data provide a possible explanation for BRMS1-associated increase in anoikis previously observed both in in vivo and in vitro studies.

However, focal adhesion assembly is only the beginning of the adhesion step-wise progression, as it leads to downstream rearrangement in microtubules

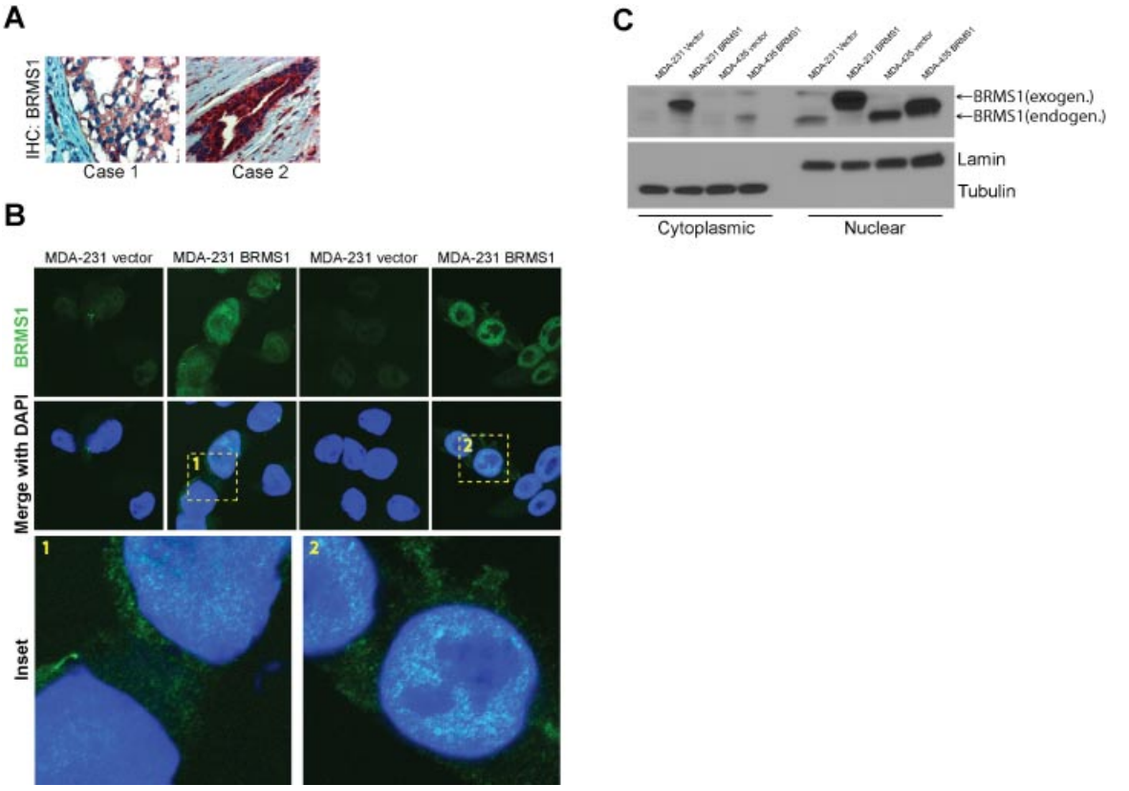

Figure 7. BRMS1 can be localized to the cytoplasm of MDA-231 and MDA-435 breast cancer cells. (A) BRMS1 expression was analyzed by immunohistochemistry (IHC) in 24 breast cancer patient samples, with several cases exhibiting strong cytoplasmic staining. (B) MDA-231 and MDA-435 vector and BRMS1-expressing cells were analyzed by confocal analysis for expression of BRMS1 (green). Nuclei were stained with DAPI (blue) for reference. (C) Cells were subjected to nuclear and cytoplasmic fractionation. Cell lysates were analyzed for BRMS1 by Western blotting.

and actin cytoskeleton. Hence, it is not surprising that expression of BRMS1 also deregulates cytoskeletal remodeling associated with cell/matrix interaction. Upon contact with the ECM, in BRMS1-expressing cells there is an adhesion-associated decrease in levels of MRTF and SRF, both of which are tightly coupled to dynamic switching of globular (destabilized) to fibrillar (stabilized) actin filaments [66,67]. In addition to BRMS1-associated actin cytoskeleton changes, we observed a similar pattern in localization and morphologic appearance of tubulin, a major component of microtubular cytoskeleton. In response to transition from round to spread cell morphology, vector control cells in an adhesion-dependent manner exhibit highly aligned microtubules that extend radial from the nucleus to the outer-most cell membrane, while BRMS1-expressing cells exhibit polarized tubulin without radial organization (Khotskaya and Welch, unpublished data). This observation holds potential importance in relation to BRMS1 and clinical progression of breast cancer. As recent publications show, tubulin can be deacetylated and thus destabilized in the cytoplasm through actions of a major cytoplasmic histone deacetylase, HDAC6 [68,69] and these post-translational modifications define its cytoskeletal activity [3]. BRMS1, known to localize and presumably function predominantly in the nucleus, associates with a number of HDAC complexes [61,62,70], including HDAC6. Surprisingly, several investigators had recently shown that BRMS1 is abundantly present in the cytosol of human cancer patient cells [60,71], yet its cytosolic function(s), if any, are unknown. Based on our observations, it is possible that BRMS1 may have some yet unknown functions in the cytoplasm, such as a direct effect on microtubules and actin filaments that results in cytoskeletal destabilization. Moreover, BRMS1 also directly associates with smoothelin, a cytoplasmic troponin-like cytoskeletal protein [62]. While smoothelin is found exclusively in contractile smooth muscle cells [72], it shares a high degree of homology with other, more ubiquitous, cytoskeletal proteins such as dystrophin and alpha-actinin [72] and its domain responsible for interacting with BRMS1 is yet unknown. Hence, it may be possible that BRMS1 plays a direct role in regulating cytoskeletal organization, either by post-translationally modifying microtubular cytoskeleton or by interacting with other cytoskeleton-associated

proteins. Follow-up studies aimed to elucidate BRMS1 function(s) in the cytoplasm are underway. Moreover, by combining data shown here with previous findings of direct interaction between BRMS1 and HDAC6, we suggest that BRMS1 expression may be used as a biomarker for selecting breast cancer patients for HDAC6 inhibitor clinical trials.

In addition to its role as a potential biomarker used for selecting patients for clinical trials, BRMS1 expression may serve as a clinical prognostic marker, capable of predicting the likelihood of disease relapse or response to targeted therapy. Specifically, recent evidence suggests that interfering with cells' ability to attach to matrix sensitizes them to cell death through TNF-related apoptosis-inducing ligand (TRAIL) pathway [73], indicating that BRMS1+ breast cancer patients may benefit from TRAIL-targeted therapy. However, one must carefully consider how to assay BRMS1 expression in the clinical setting. To date, clinical correlative data have been somewhat inconsistent, depending upon whether BRMS1 mRNA or protein were measured [74–76], its subcellular localization patterns [60], antibodies used [60,75], whether tissue samples were contaminated by stromal cells and which cells were examined [34]. The findings presented here highlight the importance of appropriate cell type selection. Data predict that assessment of BRMS1 expression in lymph node-infiltrating carcinoma cells (less than 0.2 mm or 200 cells), but not in overt metastasis, may serve as a new prognostic biomarker (Edge and American Joint Committee on Cancer, 2010). Therefore, BRMS1 may serve as a potential prognostic marker for patient relapse if expression is assayed in circulating (CTC) or disseminated tumor cells (DTC) [77,78] or in cells present in sentinel lymph nodes, that is, those cells that have already initiated the metastatic process or, as importantly, completed steps of metastasis for which BRMS1 has already been demonstrated to play lesser roles. Lombardi and colleagues recently found that breast carcinoma cells in lymph nodes expressed less BRMS1 than tumor cells from matching primary tumors, as is expected for a metastasis suppressor [74]. While their findings measured expression in overt lymph node metastases, they made no prediction for patient prognosis based on BRMS1 expression on carcinoma cells in the lymph nodes. Yet, we predict that breast cancer patients who exhibit BRMS1 expression on CTC or DTC would have a better prognosis than those without BRMS1, identifying a class of patients at a greater risk for relapse.

In summary, taking previously published data and combining it with the observations presented here, BRMS1 appears to impair cellular responses to microenvironment. Results indicate that adhesion is a dynamic process, and studying it would benefit from careful kinetics analysis. In regards to BRMS1, our data signify that BRMS1-expressing cells can adhere to multiple matrices, but not firmly. Therefore, there may be a clinical opportunity to interfere with their dissemination through anti-metastatic insults. Furthermore, expression of BRMS1 on lymph node-infiltrating carcinoma cells, CTC and DTC might serve as a biomarker, able to distinguish patients at a greater risk of relapse.

METHODS AND MATERIALS

Cell Lines and Culture

Human breast cancer cell lines MDA-MB-231 and MDA-MB-435 were obtained from Dr. Janet Price at the MD Anderson Cancer Center (described in Ref. [79,80]) and engineered to stably express BRMS1 (pooled cell population, Figure 2A) or empty expression vector as described previously [55,61]. Cells were cultured in Dulbecco's-modified Eagle's medium mixed 1:1 (v:v) with Ham's F-12 medium (DMEM/F12, #11330, Invitrogen, Carlsbad, CA) supplemented with 5% fetal bovine serum (FBS, Atlanta Biologicals, Lawrenceville, GA), 2 mmol/L of L-glutamine (Invitrogen), and 0.02 mmol/L of non-essential amino acids (Mediatech, Manassas, VA). Neither antibiotics nor anti-mycotics were used. All cell lines were tested and found to be negative of *Mycoplasma* spp. contamination, using a PCR-based kit (#302108; Aligent Technologies, Santa Clara, CA). Cells were routinely passaged using 0.2 mmol/L EDTA in Ca^{2+}-free, Mg^{2+}-free, and $NaHCO_3$-free Hank's balanced salt solution (Invitrogen). Following breast cancer cell lines were obtained from ATCC and cultured as previously described: SKBR3, HBL100, Hs578, MDA-468, MDA-436, MDA-361, ZR75-1, 4T1, MCF10F, MCF10A. All cell lines were fingerprinted by the MDACC Institutional Core Facility, and their identity confirmed and identical to ATCC cell line profiles based on 13 identification criteria.

Antibodies

Active β1 integrin (# MAB2079Z, Millipore, Billerica, MA), Tubulin (#2125, Cell Signaling, Danvers, MA), Integrin Signaling Kit to test expression of α4, α5, αV, β1, β3, β4, and β5 integrins (#4749, Cell Signaling), pFAK Y397 (#44624G, Invitrogen), Talin1 (#05-1144, Millipore), Actin Cytoskeleton and Focal Adhesion Staining Kit for immunofluorescence of actin and Vinculin (#FAK100, Millipore), total FAK (#3285, Cell Signaling), ILK (#3862, Cell Signaling), MRTF (#A302-201A, Bethyl Labs, Montgomery, TX), SRF (#sc-335, Santa Cruz Biotechnology, Santa Cruz, CA), Small GTPase Kit to test expression of RhoA, RhoB, and RhoC (#9968, Cell Signaling), anti-mouse-FITC IgG (#F-2761, Molecular Probes of Invitrogen), anti-rabbit-FITC IgG (#F-2765, Molecular Probes of Invitrogen), anti-mouse IgG with peroxidase (#NXA931, Amersham, Piscataway, NJ), anti-rabbit IgG with peroxidase (#NA934, Amersham). Monoclonal BRMS1 antibody 1a5.7 was described previously [61]. BRMS1 antibody used for immunofluorescence

was from Abcam (#ab134968, Abcam, Cambridge, MA).

Western Blot

Western blotting was performed as described previously [81]. Briefly, cells were lysed in RIPA buffer (25 mM Tris–HCL pH 7.6, 150 mM NaCl, 1% NP-40, 1% sodium deoxycholate, and 0.1% SDS, supplemented with protease and phosphatase inhibitors), and protein concentrations approximated with BCA assay (Pierce, Rockford, IL). Cell lysates were resolved on precast 4–15% SDS–PAGE (BioRad, Hercules, CA) under constant voltage conditions. Gels were blotted onto PVDF membrane and blocked in 5% non-fat dry milk. Membranes were incubated in primary antibody overnight at 4°C. Following incubation with the secondary antibody, membranes were developed using chemiluminescent substrate kit (Pierce). Signal was detected by exposing membranes to X-ray film. Band intensity was analyzed by densitometry using NIH ImageJ software, and all experiments were done in triplicate.

Cell Proliferation

75 000 cells were plated per well of a 6-well plate in triplicate in DMEM/F-12 media supplemented with 5% FBS. At times indicated, cells were trypsinized and manually counted to assess proliferation rate.

Anoikis Assay

100 000 cells were plated per well of a 6-well ultra-low adhesion plate (Corning) in DMEM/F-12 media supplemented with 5% FBS, which maintained cells in a suspension culture. At times indicated, cell aliquots were taken and cells manually counted to assess anoikis rate based on trypan blue exclusion method.

BRMS1 Immunohistochemistry on Breast Cancer Patient Tissues

BRMS1 immunohistochemistry was performed as previously described [60] under Institutional Review Board-approved protocol.

3D Collagen I Culture

3D collagen I culture kit was purchased from Millipore (#ECM675, Millipore) and experiments performed as per kit's instructions. Briefly, for confocal experiments cells were suspended in collagen I to 50 000 cells/mL final concentration and 50 μL of cell suspension added per well of 8-well chamber slide (#177445, Nunc, Rochester, NY). At times indicated, cells were fixed within collagen gels and immunofluorescence staining performed as per kit instructions. For long-term culture, cells were diluted in collagen I to 100 000 cells/mL final concentration and 0.5 mL plated per well of 12-well plates. After gels solidified, regular growth media was added and replaced every 2 d. After 7–10 d of culture, five non-overlapping areas were examined, photographed using CarlZeiss inverted Stemi 2000-C microscope (Axiovision software package) and at least 150 colonies counted. Invasive colonies were defined as consisting of more that four cells migrating away from their structure of origin [82]. To collect cell lysates, collagen I gels were digested with collagenase type I from *Clostridium histolyticum* (#SCR103, Millipore), cells pelleted by centrifugation, and lysed for Western blotting analysis following procedure previously described [81].

3D Matrigel Culture

Growth factor reduced Matrigel was purchased from BD Biosciences (#256231, BD Biosciences, San Jose, CA). Cell culture plates were coated with 150 μL Matrigel per well of 24-well plate and then placed at 37°C for 5 min. Cells were diluted to 1000 cells/mL in complete culture medium supplemented with 10% FBS and kept on ice. Immediately prior to plating, Matrigel was added to cell suspension to achieve 2% final Matrigel concentration. After plating, cultures were moved into an incubator and cultured for 14 d at 37°C. Media was changed every 3–4 d. After 12 d of culture, five non-overlapping areas were examined, photographed using CarlZeiss inverted Stemi 2000-C microscope (Axiovision software package) and colonies counted.

Adhesion Assay

6-well culture plates (Nunc Nalgene) were coated with 1 mL of whole undiluted FBS, collagen I from human lung (final concentration 50 μg/mL, Sigma–Aldrich, St. Louis, MO), collagen IV from human placenta (final concentration 50 μg/mL, Sigma–Aldrich), or fibronectin from human plasma (final concentration 50 μg/mL, Sigma–Aldrich) overnight on a rocker at 4°C. The following day, matrix solution was aspirated, plates washed three times with ice-cold phosphate buffered saline (PBS), and allowed to air dry. Breast cancer cells were serum-starved for 24 h prior to onset of adhesion studies to exclude growth factor-mediated adhesion events. Cells were suspended in serum-free DMEM/F12 and suspension added to precoated plates for time intervals indicated. Non-adhered cells were washed off with two quick PBS washes with manual agitation. Adherent cells were lysed in RIPA buffer for Western blotting analysis following protocol described above or fixed for immunofluorescence staining. For crystal violet staining, adherent cells were fixed with 4% formaldehyde in PBS, stained with dye solution, followed by several washes with water. Crystal violet adhesion experiment was done in triplicate, at least five non-overlapping areas were examined per replicate, photographed using CarlZeiss inverted Stemi 2000-C microscope (Axiovision software package) and at least 120 adherent cells counted, except for MDA-435 and MDA-435-BRMS1 cells at 5 min, where only 50 cells were counted due to low adhesion rate. To

measure cell length, all images were scaled and cell diameter measured using ImageJ ROI tool. At least 120 cells were measured.

Immunofluorescence and Confocal Microscopy

Cells were plated on FBS-coated 8-well chamber slides (Nunc) and allowed to adhere for times indicated. Non-adhered cells were washed off with PBS. Cells were fixed with 4% formaldehyde in PBS, permeabilized with 0.5% Triton-X100, blocked against non-specific antigens with 5% bovine serum albumin (BSA) in PBS, and incubated overnight at 4°C with primary antibody dilution. Following incubation with the fluoropore-conjugated secondary antibody, slides were mounted with DAPI-containing hard-set media (Vectashield, Vector Labs, Burlingame, CA). Cells were examined on CarlZeiss LSM 710 confocal microscope with ZEN 2009 software.

Time-Lapse Microscopy

For 2D imaging, cells were added to precoated plates under the microscope and imaging started immediately. Photographic images were taken every 15 s for 1 h total. For 3D culture imaging, gels were allowed to set in tissue culture incubator for 1 h, then serum-free or serum-containing media was added (as indicated) and at least five non-overlapping areas of the gel chosen for observation. Photographic images were taken every 15 min for 48 h total. All time-lapse microscopy was performed on CarlZeiss Cell Observer microscope running Axiovision software package and equipped with CO_2 chamber and 37°C warm plate.

BRMS1 Knockdown

Lentiviral vectors containing BRMS1-targeting shRNA sequences were purchased from MD Anderson ORF and shRNA core facility. Upon infection with lentivirus, stable cells were selected with puromycin. For an unknown reason, BRMS1 knockdown was very unstable in MDA-231-BRMS1-expressing cells and cells regained BRMS1 expression within 2 wk of culture. BRMS1 knockdown could not be achieved in MDA-435 cells.

Statistical Analysis

Statistical analyses were performed using Student's *t*-test and $P < 0.05$ was deemed significant.

ACKNOWLEDGMENTS

Y.B.K. was supported in part through NCI-Supported Ruth L. Kirchstein Institutional (T32) National Research Service Award granted to the University of Alabama at Birmingham Center for Metabolic Bone Diseases (Postdoctoral Fellowship Award AR047512-08) and Department of Defense (DOD) Congressionally Directed Medical Research Breast Cancer Research Program (Postdoctoral Fellowship Award W81XWH-10-1-0749). D.R.H. is supported by the American Cancer Society (Award RSG-11-259-01-CSM). D.R.W. is supported by National Foundation for Cancer Research Center for Metastasis Research, National Institute of Health (RO1-CA87728; RO1-CA134981; and P30-CA168524), and Susan G. Komen for the Cure (Award SAC11037). M.-C.H. is supported by The University of Texas MD Anderson-China Medical University and Hospital Sister Institution Fund, MD Anderson Cancer Center Support Grant (Award CA16672), MD Anderson Center for Biological Pathways; National Breast Cancer Foundation, Inc.; Program for Stem Cell and Regenerative Medicine Frontier Research (NSC101-2321-B-039-001, Taiwan); International Research-Intensive Centers of Excellence in Taiwan (NSC102-2911-I-002-303); and Cancer Research Center of Excellence (DOH102-TD-C-111-005, Taiwan). We thank Dr. Mariano Ponz Sarvise and Mr. Shih-Shin Chang for their helpful comments and fruitful discussions.

REFERENCES

1. Fidler IJ, Kripke ML. Metastasis results from preexisting variant cells within a malignant tumor. Science 1977;197: 893–895.
2. Fidler IJ. Metastasis: guantitative analysis of distribution and fate of tumor embolilabeled with 125 I-5-iodo-2'-deoxyuridine. J Natl Cancer Inst 1970;45:773–782.
3. Zilberman Y, Ballestrem C, Carramusa L, et al. Regulation of microtubule dynamics by inhibition of the tubulin deacetylase HDAC6. J Cell Sci 2009;122:3531–3541.
4. Eccles SA, Welch DR. Metastasis: Recent discoveries and novel treatment strategies. Lancet 2007;369:1742–1757.
5. Chaffer CL, Weinberg RA. A perspective on cancer cell metastasis. Science 2011;331:1559–1564.
6. Hanahan D, Weinberg RA. Hallmarks of cancer: The next generation. Cell 2011;144:646–674.
7. Nagaprashantha LD, Vatsyayan R, Lelsani PC, Awasthi S, Singhal SS. The sensors and regulators of cell-matrix surveillance in anoikis resistance of tumors. Int J Cancer 2011;128: 743–752.
8. Gupta GP, Massague J. Cancer metastasis: Building a framework. Cell 2006;127:679–695.
9. Weiss L, Mayhew E, Rapp DG, Holmes JC. Metastatic inefficiency in mice bearing B16 melanomas. Br J Cancer 1982;45:44–53.
10. Loeffler M, Kruger JA, Niethammer AG, Reisfeld RA. Targeting tumor-associated fibroblasts improves cancer chemotherapy by increasing intratumoral drug uptake. J Clin Invest 2006;116:1955–1962.
11. Dornhofer N, Spong S, Bennewith K, et al. Connective tissue growth factor-specific monoclonal antibody therapy inhibits pancreatic tumor growth and metastasis. Cancer Res 2006;66:5816–5827.
12. Erler JT, Bennewith KL, Nicolau M, et al. Lysyl oxidase is essential for hypoxia-induced metastasis. Nature 2006;440: 1222–1226.
13. Barkan D, Green JE, Chambers AF. Extracellular matrix: A gatekeeper in the transition from dormancy to metastatic growth. Eur J Cancer 2010;46:1181–1188.
14. Schwock J, Dhani N, Hedley DW. Targeting focal adhesion kinase signaling in tumor growth and metastasis. Expert Opin Ther Targets 2010;14:77–94.
15. Eble JA, Niland S. The extracellular matrix of blood vessels. Curr Pharm Des 2009;15:1385–1400.

16. Khotskaya YB, Dai Y, Ritchie JP, et al. Syndecan-1 is required for robust growth, vascularization, and metastasis of myeloma tumors in vivo. J Biol Chem 2009;284:26085–26095.
17. Nelson CM, Bissell MJ. Modeling dynamic reciprocity: Engineering three-dimensional culture models of breast architecture, function, and neoplastic transformation. Semin Cancer Biol 2005;15:342–352.
18. Slorach EM, Chou J, Werb Z. Zeppo1 is a novel metastasis promoter that represses E-cadherin expression and regulates p120-catenin isoform expression and localization. Genes Dev 2011;25:471–484.
19. Ewald AJ, Werb Z, Egeblad M. Dynamic, long-term in vivo imaging of tumor-stroma interactions in mouse models of breast cancer using spinning-disk confocal microscopy. Cold Spring Harb Protoc 2011;2:122–137.
20. Condeelis J, Weissleder R. In vivo imaging in cancer. Cold Spring Harb Perspect Biol 2010;2:a003848.
21. Patsialou A, Wyckoff J, Wang Y, et al. Invasion of human breast cancer cells in vivo requires both paracrine and autocrine loops involving the colony-stimulating factor-1 receptor. Cancer Res 2009;69:9498–9506.
22. Xue C, Wyckoff J, Liang F, et al. Epidermal growth factor receptor overexpression results in increased tumor cell motility in vivo coordinately with enhanced intravasation and metastasis. Cancer Res 2006;66:192–197.
23. Wyckoff JB, Jones JG, Condeelis JS, Segall JE. A critical step in metastasis: In vivo analysis of intravasation at the primary tumor. Cancer Res 2000;60:2504–2511.
24. Borsig L, Vlodavsky I, Ishai-Michaeli R, Torri G, Vismara E. Sulfated hexasaccharides attenuate metastasis by inhibition of P-selectin and heparanase. Neoplasia 2011;13:445–452.
25. Finger EC, Giaccia AJ. Hypoxia, inflammation, and the tumor microenvironment in metastatic disease. Cancer Metastasis Rev 2010;29:285–293.
26. Boimel PJ, Smirnova T, Zhou ZN, et al. Contribution of CXCL12 secretion to invasion of breast cancer cells. Breast Cancer Res 2012;14:R23.
27. Gonda K, Watanabe TM, Ohuchi N, Higuchi H. In vivo nano-imaging of membrane dynamics in metastatic tumor cells using quantum dots. J Biol Chem 2010;285:2750–2757.
28. Pierga JY, Hajage D, Bachelot T, et al. High independent prognostic and predictive value of circulating tumor cells compared with serum tumor markers in a large prospective trial in first-line chemotherapy for metastatic breast cancer patients. Ann Oncol 2011;3:618–624.
29. Riethdorf S, Fritsche H, Muller V, et al. Detection of circulating tumor cells in peripheral blood of patients with metastatic breast cancer: A validation study of the CellSearch system. Clin Cancer Res 2007;13:920–928.
30. Pantel K, Alix-Panabieres C. The clinical significance of circulating tumor cells. Nat Clin Pract Oncol 2007;4:62–63.
31. Wang W, Luo BH. Structural basis of integrin transmembrane activation. J Cell Biochem 2010;109:447–452.
32. Carman CV. Overview: Imaging in the study of integrins. Methods Mol Biol 2012;757:159–189.
33. Maruthamuthu V, Aratyn-Schaus Y, Gardel ML. Conserved F-actin dynamics and force transmission at cell adhesions. Curr Opin Cell Biol 2010;22:583–588.
34. Olson EN, Nordheim A. Linking actin dynamics and gene transcription to drive cellular motile functions. Nat Rev Mol Cell Biol 2010;11:353–365.
35. Shattil SJ, Kim C, Ginsberg MH. The final steps of integrin activation: The end game. Nat Rev Mol Cell Biol 2010;11:288–300.
36. Partridge MA, Marcantonio EE. Initiation of attachment and generation of mature focal adhesions by integrin-containing filopodia in cell spreading. Mol Biol Cell 2006;17:4237–4248.
37. Li Y, Fan ZC, Guo J, et al. Circulation times of hepatocellular carcinoma cells by in vivo flow cytometry. Chin Opt Lett 2010;8:953–956.
38. Georgakoudi I, Solban N, Novak J, et al. In vivo flow cytometry: A new method for enumerating circulating cancer cells. Cancer Res 2004;64:5044–5047.
39. Digman MAJ, Gratton E, Suetsugu A, Hoffman RM. *Real-time imaging of 3-dimensional cancer cell movement in tissues*. San Diego, CA: University of California San Diego; 2011.
40. Torres VA, Stupack DG. Rab5 in the regulation of cell motility and invasion. Curr Protein Pept Sci 2011;12:43–51.
41. Zhao B, Li L, Wang L, et al. Cell detachment activates the Hippo pathway via cytoskeleton reorganization to induce anoikis. Genes Dev 2012;26:54–68.
42. Madsen CD, Sahai E. Cancer dissemination—Lessons from leukocytes. Dev Cell 2010;19:13–26.
43. Muller WA. Mechanisms of leukocyte transendothelial migration. Annu Rev Pathol 2011;6:323–344.
44. Alon R, Chen S, Puri KD, Finger EB, Springer TA. The kinetics of L-selectin tethers and the mechanics of selectin-mediated rolling. J Cell Biol 1997;138:1169–1180.
45. Salas A, Shimaoka M, Chen SQ, Carman CV, Springer T. Transition from rolling to firm adhesion is regulated by the conformation of the I domain of the integrin lymphocyte function-associated antigen-1. J Biol Chem 2002;277:50255–50262.
46. Fernandez-Borja M, van Buul JD, Hordijk PL. The regulation of leucocyte transendothelial migration by endothelial signalling events. Cardiovasc Res 2010;86:202–210.
47. McEver RP. Rolling back neutrophil adhesion. Nat Immunol 2010;11:282–284.
48. Springer TA. The sensation and regulation of interactions with the extracellular environment: The cell biology of lymphocyte adhesion receptors. Annu Rev Cell Biol 1990;6:359–402.
49. Carman CV, Sage PT, Sciuto TE, et al. Transcellular diapedesis is initiated by invasive podosomes. Immunity 2007;26:784–797.
50. Carman CV, Springer TA. Trans-cellular migration: Cell–cell contacts get intimate. Curr Opin Cell Biol 2008;20:533–540.
51. Chambers AF. MDA-MB-435 and M14 cell lines: Identical but not M14 melanoma? Cancer Res 2009;69:5292–5293.
52. Sellappan S, Grijalva R, Zhou X, et al. Lineage infidelity of MDA-MB-435 cells: Expression of melanocyte proteins in a breast cancer cell line. Cancer Res 2004;64:3479–3485.
53. Hurst DR, Welch DR. Metastasis suppressor genes at the interface between the environment and tumor cell growth. Int Rev Cell Mol Biol 2011;286:107–180.
54. Hedley BD, Vaidya KS, Phadke P, et al. BRMS1 suppresses breast cancer metastasis in multiple experimental models of metastasis by reducing solitary cell survival and inhibiting growth initiation. Clin Exp Metastasis 2008;25:727–740.
55. Phadke PA, Vaidya KS, Nash KT, Hurst DR, Welch DR. BRMS1 suppresses breast cancer experimental metastasis to multiple organs by inhibiting several steps of the metastatic process. Am J Pathol 2008;172:809–817.
56. Hedley BD, Welch DR, Allan AL, et al. Downregulation of osteopontin contributes to metastasis suppression by breast cancer metastasis suppressor 1. Int J Cancer 2008;123:526–534.
57. Samant RS, Seraj MJ, Saunders MM, et al. Analysis of mechanisms underlying BRMS1 suppression of metastasis. Clin Exp Metastasis 2000;18:683–693.
58. Lynch CD, Lazar AM, Iskratsch T, Zhang X, Sheetz MP. Endoplasmic spreading requires coalescence of vimentin intermediate filaments at force-bearing adhesions. Mol Biol Cell 2013;24:21–30.
59. Kaab MJ, Gwynn IA, Notzli HP. Collagen fibre arrangement in the tibial plateau articular cartilage of man and other mammalian species. J Anat 1998;193:23–34.
60. Frolova N, Edmonds MD, Bodenstine TM, et al. A shift from nuclear to cytoplasmic breast cancer metastasis suppressor 1 expression is associated with highly proliferative estrogen receptor-negative breast cancers. Tumour Biol 2009;30:148–159.

61. Hurst DR, Xie Y, Vaidya KS, et al. Alterations of BRMS1-ARID4A interaction modify gene expression but still suppress metastasis in human breast cancer cells. J Biol Chem 2008;283:7438–7444.
62. Hurst DR, Mehta A, Moore BP, et al. Breast cancer metastasis suppressor 1 (BRMS1) is stabilized by the Hsp90 chaperone. Biochem Biophys Res Commun 2006;348:1429–1435.
63. Hurst DR, Welch DR. Unraveling the enigmatic complexities of BRMS1-mediated metastasis suppression. FEBS Lett 2011;585: 3185–3190.
64. Heyder C, Gloria-Maercker E, Entschladen F, et al. Realtime visualization of tumor cell/endothelial cell interactions during transmigration across the endothelial barrier. J Cancer Res Clin Oncol 2002;128:533–538.
65. Krishnan V, Shuman LA, Sosnoski DM, et al. Dynamic interaction between breast cancer cells and osteoblastic tissue: Comparison of two- and three-dimensional cultures. J Cell Physiol 2011;226:2150–2158.
66. Leitner L, Shaposhnikov D, Mengel A, et al. MAL/MRTF-A controls migration of non-invasive cells by upregulation of cytoskeleton-associated proteins. J Cell Sci 2011;124:4318–4331.
67. Rey M, Irondelle M, Waharte F, Lizarraga F, Chavrier P. HDAC6 is required for invadopodia activity and invasion by breast tumor cells. Eur J Cell Biol 2011;90:128–135.
68. Zhang Y, Li N, Caron C, et al. HDAC-6 interacts with and deacetylates tubulin and microtubules in vivo. EMBO J 2003;22:1168–1179.
69. Meehan WJ, Samant RS, Hopper JE, et al. Breast cancer metastasis suppressor 1 (BRMS1) forms complexes with retinoblastoma-binding protein 1 (RBP1) and the mSin3 histone deacetylase complex and represses transcription. J Biol Chem 2004;279:1562–1569.
70. Nagji AS, Liu Y, Stelow EB, Stukenborg GJ, Jones DR. BRMS1 transcriptional repression correlates with CpG island methylation and advanced pathological stage in non-small cell lung cancer. J Pathol 2010;221:229–237.
71. van der Loop FT, Schaart G, Timmer ED, Ramaekers FC, van Eys GJ. Smoothelin, a novel cytoskeletal protein specific for smooth muscle cells. J Cell Biol 1996;134:401–411.
72. Phipps LE, Hino S, Muschel RJ. Targeting cell spreading: A method of sensitizing metastatic tumor cells to TRAIL-induced apoptosis. Mol Cancer Res 2011;9:249–258.
73. Lombardi G, Di Cristofano C, Capodanno A, et al. High level of messenger RNA for BRMS1 in primary breast carcinomas is associated with poor prognosis. Int J Cancer 2007;120:1169–1178.
74. Hicks DG, Yoder BJ, Short S, et al. Loss of breast cancer metastasis suppressor 1 protein expression predicts reduced disease-free survival in subsets of breast cancer patients. Clin Cancer Res 2006;12:6702–6708.
75. Zhang Z, Yamashita H, Toyama T, et al. Reduced expression of the breast cancer metastasis suppressor 1 mRNA is correlated with poor progress in breast cancer. Clin Cancer Res 2006;12:6410–6414.
76. Kelly LM, Buggy Y, Hill A, et al. Expression of the breast cancer metastasis suppressor gene, BRMS1, in human breast carcinoma: Lack of correlation with metastasis to axillary lymph nodes. Tumour Biol 2005;26:213–216.
77. Pantel K, Alix-Panabieres C, Riethdorf S. Cancer micrometastases. Nat Rev Clin Oncol 2009;6:339–351.
78. Pantel K, Riethdorf S. Pathology: Are circulating tumor cells predictive of overall survival? Nat Rev Clin Oncol 2009;6:190–191.
79. Price JE, Polyzos A, Zhang RD, Daniels LM. Tumorigenicity and metastasis of human breast carcinoma cell lines in nude mice. Cancer Res 1990;50:717–721.
80. Zhang RD, Fidler IJ, Price JE. Relative malignant potential of human breast carcinoma cell lines established from pleural effusions and a brain metastasis. Invasion Metastasis 1991;11:204–215.
81. Vaidya KS, Harihar S, Phadke PA, et al. Breast cancer metastasis suppressor-1 differentially modulates growth factor signaling. J Biol Chem 2008;283:28354–28360.
82. Jedeszko C, Victor BC, Podgorski I, Sloane BF. Fibroblast hepatocyte growth factor promotes invasion of human mammary ductal carcinoma in situ. Cancer Res 2009;69: 9148–9155.

SUPPORTING INFORMATION

Additional supporting information may be found in the online version of this article at the publisher's web-site.

Figure 1. BRMS1 expression does not affect cell proliferation rate. (A) Proliferation of vector and BRMS1-expressing cells was measured by manual cell counting over 4 d. Data are mean of triplicate experiments ± SEM. (B) BRMS1 expression was assayed by Western blotting in lysates from vector and BRMS1-transfected cells, as well as in lysates from wild-type, untransfected cells.

Figure 2. Expression of BRMS1 reduces integrin activation and localization to areas of focal contact. Vector control and BRMS1-expressing cells were plated onto chamber slides precoated with FBS and allowed to adhere for 30 min. Fixed cells were stained for actin (red) and activated β1 integrin (green). Nuclei were stained with DAPI (blue) for reference. Scale bar = 20 μm. At least three non-overlapping view areas were examined and each experiment repeated at least twice.

Figure 3. Expression of BRMS1 reduces spreading of cells on ECM components. Vector control and BRMS1-expressing cells were plated onto chamber slides precoated with collagen I, collagen IV, or fibronectin and allowed to adhere for 30 min. Fixed cells were stained for pFAK (green) to indicate focal adhesions. Nuclei were stained with DAPI (blue) for reference. Scale bar = 20 μm. At least three nonoverlapping view areas were examined and each experiment repeated at least twice.

Figure 4. Expression of BRMS1 reduces localization of activated β1 integrin to focal adhesions when cells are plated on ECM components. Vector control and BRMS1-expressing cells were plated onto chamber slides precoated with collagen I, collagen IV, or fibronectin and allowed to adhere for 30 min. Fixed cells were stained for activated β1 integrin (green) to indicate focal adhesions. Nuclei were stained with DAPI (blue) for reference. Scale bar = 20 μm. At least three non-overlapping view areas were examined and each experiment repeated at least twice.

Movies 1–4. BRMS1 delays adhesion of MDA-231 and MDA-435 breast cancer cells. Vector control and BRMS1-expressing breast cancer cells were plated

onto optical plates precoated with whole FBS and imaged in live cell time-lapse mode for 1 h. At least five non-overlapping view areas were imaged and analyzed.

Movies 5–8. BRMS1-expressing breast cancer cells interact with 3D collagen I matrix less when compared to vector control cells. Vector control and BRMS1-expressing breast cancer cells were plated in 3D collagen I and imaged in live cell time-lapse mode for 48 h. At least five non-overlapping view areas were imaged and analyzed, and experiments were repeated twice.